Published as: *J Neurophysiol*. 2002 June ; 87(6): 2684–2699.

# Role of Arcuate Frontal Cortex of Monkeys in Smooth Pursuit Eye Movements. I. Basic Response Properties to Retinal Image Motion and Position

**Masaki Tanaka** and **Stephen G. Lisberger**
*Howard Hughes Medical Institute, Department of Physiology and W. M. Keck Foundation Center for Integrative Neuroscience, University of California, San Francisco, California 94143*

## Abstract

Anatomical and physiological studies have shown that the "frontal pursuit area" (FPA) in the arcuate cortex of monkeys is involved in the control of smooth pursuit eye movements. To further analyze the signals carried by the FPA, we examined the activity of pursuit-related neurons recorded from a discrete region near the arcuate spur during a variety of oculomotor tasks. Pursuit neurons showed direction tuning with a wide range of preferred directions and a mean full width at half-maximum of 129°. Analysis of latency using the "receiver operating characteristic" to compare responses to target motion in opposite directions showed that the directional response of 58% of FPA neurons led the initiation of pursuit, while 19% led by 25 ms or more. Analysis of neuronal responses during pursuit of a range of target velocities revealed that the sensitivity to eye velocity was larger during the initiation of pursuit than during the maintenance of pursuit, consistent with two components of firing related to image motion and eye motion. FPA neurons showed correlates of two behavioral features of pursuit documented in prior reports. *1*) Eye acceleration at the initiation of pursuit declines as a function of the eccentricity of the moving target. FPA neurons show decreased firing at the initiation of pursuit in parallel with the decline in eye acceleration. This finding is consistent with prior suggestions that the FPA plays a role in modulating the gain of visual-motor transmission for pursuit. *2*) A stationary eccentric cue evokes a smooth eye movement opposite in direction to the cue and enhances the pursuit evoked by subsequent target motions. Many pursuit neurons in the FPA showed weak, phasic visual responses for stationary targets and were tuned for the positions about 4° eccentric on the side opposite to the preferred pursuit direction. However, few neurons (12%) responded during the preparation or execution of saccades. The responses to the stationary target could account for the behavioral effects of stationary, eccentric cues. Further analysis of the relationship between firing rate and retinal position error during pursuit in the preferred and opposite directions failed to provide evidence for a large contribution of image position to the firing of FPA neurons. We conclude that FPA processes information in terms of image and eye velocity and that it is functionally separate from the saccadic frontal eye fields, which processes information in terms of retinal image position.

## INTRODUCTION

Smooth pursuit is a voluntary eye movement that allows primates to track a slowly moving object with excellent accuracy. Much is already known about the neuronal substrates for smooth pursuit (for reviews see: Eckmiller 1987; Keller and Heinen 1991; Leigh and Zee 1991; Lisberger et al. 1987). Its sensory input is visual motion that is extracted and processed

Present address and address for reprint requests: M. Tanaka, Dept. of Physiology, Hokkaido University School of Medicine, North 15, West 7, Sapporo 060-8638, Japan (E-mail: masaki@med.hokudai.ac.jp).

through the dorsal visual pathways in the cerebral cortex, including the middle temporal area (MT) and the medial superior temporal area (MST). Neurons in MT and MST, in turn, project via a synapse in the pontine nuclei to the cerebellum, providing a direct parieto-ponto-cerebellar pathway that seems to provide signals responsible for the visual guidance of pursuit (Keller and Heinen 1991; Lisberger et al. 1987).

The present pair of papers concerns a region of the frontal cortex that has recently been added to the list of the neuronal substrates for pursuit. The posterior part of the arcuate sulcus, which we refer to as the "frontal pursuit area" (FPA), contains neurons that discharge during pursuit, but not during saccades (Gottlieb et al. 1994; Tanaka and Fukushima 1998). Lesion studies have shown that the FPA is necessary for normal pursuit performance (Keating 1991, 1993; Lynch 1987; MacAvoy et al. 1991; Shi et al. 1998), while stimulation studies have shown that the output from the FPA has access to the pursuit system (Gottlieb et al. 1993; Tanaka and Lisberger 2001, 2002; Tian and Lynch 1996a). Anatomical studies have raised the possibility that the FPA is part of a circuit that processes information in parallel with the direct parieto-ponto-cerebellar circuit. The periarcuate cortex does have reciprocal connections with the dorsal visual pathways including MT, MST, and the lateral and the ventral intraparietal areas (e.g., Huerta et al. 1987; Stanton et al. 1995; Tian and Lynch 1996b): it could contribute to or modulate the parieto-ponto-cerebellar pathways. However, anatomical studies in the *Cebus* monkeys have shown that the connectivity of the FPA is quite different from that of the parietal cortex. Large portions of the ascending inputs to the FPA originate from thalamic nuclei that are targets of the basal ganglia and cerebellar outputs (Tian and Lynch 1997). Further, the FPA projects abundantly to the putamen as well as the caudate nucleus (Cui et al. 2000, 2001). Finally, at least in *Cebus* monkeys, the outputs of the frontal pursuit area project to the dorsomedial pontine nucleus (Yan et al. 1999, 2001a), rather than to the dorsolateral pontine nucleus that serves as a relay for the parieto-ponto-cerebellar pathways.

Until recently, the FPA seemed to be an area of motor cortex that provided a neural representation of the direction of pursuit to assist in the guidance of eye velocity. However, the anatomical relationship between the FPA and the basal ganglia, and the difference in connectivity between frontal and parietal circuits, suggests that the FPA may process different information for control of pursuit than do the parietal areas. In addition, two intriguing issues have been raised by recent research. First, the close proximity of the FPA to the saccadic frontal eye fields (FEFs) raises the question of whether the FPA should be considered as a foveal extension of the FEF, or as a functionally separate area. The former view seems to hold for the superior colliculus, where the rostral pole has been suggested to have a role in pursuit (Basso et al. 2000; Krauzlis et al. 1997, 2000), but is considered to be a foveal extension of the remainder of the structure. The first paper in the present pair provides evidence that supports the latter view for the FPA and the FEF. Second, recent studies in our laboratory have provided evidence for a number of features of pursuit that would be candidates to be mediated in the FPA. Features relevant to the present series of two papers include: on-line gain control (Schwartz and Lisberger 1994), smooth eye movements evoked by a stationary eccentric visual cue (Tanaka and Lisberger 2000), vector averaging for double-target stimuli (Lisberger and Ferrera 1997), and postsaccadic enhancement of pursuit (Lisberger 1998). In the present paper, we provide neural recordings that are relevant to the neural localization of two of these features.

## METHODS

### Animal preparation

Experiments were conducted on two male rhesus monkeys (*Macaca mulatta, monkeys PCK* and *OLV*) using procedures that had been approved in advance by the Institutional Animal Care and Use Committee of the University of California, San Francisco. The same animals had been used for earlier behavioral and stimulation experiments (Tanaka and Lisberger 2000–2002).

The procedures for animal preparation were described previously (Lisberger and Westbrook 1985; Tanaka and Lisberger 2001). Briefly, after the initial training on a bar press task, a head holder and a scleral search coil were implanted in separate surgeries under isoflurane anesthesia and using sterile procedures. During the subsequent training or experimental sessions, the monkey's head was secured to the ceiling of the primate chair, and horizontal and vertical eye position were recorded using the search coil technique (Fuchs and Robinson 1966). After training in oculomotor tasks and behavioral experiments that lasted several months, a stainless steel cylinder was implanted using the same surgical procedures. The cylinder was placed over the arcuate sulcus angled 30–31° from the saggital plane, to allow electrode penetrations roughly perpendicular to the intact dura.

During times when experiments were run, we restricted the monkeys' water intake so that they were motivated to perform oculomotor tasks. The amount of water intake was measured daily, and the weight of each animal was recorded before each training or experimental session. The monkeys' health was evaluated regularly by experimenters and UCSF veterinarians and nurses.

### Visual stimulus and behavioral paradigms

Visual stimuli were presented on an analog oscilloscope (Hewlett Packard 1304A) located 28 cm away from the eyes. The oscilloscope subtended 42 × 36° of visual angle, and was controlled by a digital signal processing (DSP) board inside Pentium PC computer. The high resolution of the DSP board created a display with nominal spatial resolution of 64K pixels in each dimension and a refresh rate of 250 Hz. A 0.2° diam, white spot (3.8 cd/$m^2$) served as a visual stimulus. All experiments were carried out in a nearly dark room. The horizontal and vertical eye position signals were calibrated by having the animals fixate stationary targets at known eccentricities along the horizontal and vertical meridians. Thereafter, eye position was compared with target position, and the animal was rewarded with drops of water or juice for maintaining eye position within a window that surrounded target position throughout each trial. The trial was aborted and followed by a newly selected trial if the monkey failed to maintain eye position within the specified window.

Two behavioral paradigms were used: saccade tasks and pursuit tasks. Each trial began with the appearance of a stationary target for a random-duration fixation period that ranged from 1,000 to 1,500 ms. The fixation target was at the center of the screen in most pursuit trials and all saccade trials: deviations from this situation will be described at the relevant places in RESULTS. The direction of target motion was one of eight radial directions including the four cardinal directions and the four 45° oblique directions.

**SACCADE TASK—**After the initial fixation period, the target jumped in one direction, then remained stationary for 1,500 ms. The amplitude of target step ranged from 0.5–16°, and its direction was along the preferred axis of the neuron under study. Monkeys were required to maintain fixation within 1° of target position before the target step. The requirements for eye position were suspended for 400–600 ms after the target step, after which the monkeys were required to keep eye position within 3–4° of the target for the remainder of the trial. In a variant of the saccade task, we used an overlap paradigm where the fixation target was not extinguished until 300 ms after the appearance of the peripheral target. The animals were required to maintain eye position within 1° of the fixation target as long as it was visible. Otherwise the trial was aborted. These contingencies allowed monkeys to predict the offset of the fixation point and complete some trials successfully with early saccades. Since the purpose of the overlap task was only to delay saccades beyond the usual latency of 200 ms, we made no attempt to discourage this behavior.

**PURSUIT TASK—**Pursuit trials provided step-ramp target motion (Rashbass 1961): for most experiments, the fixation target jumped in one direction, then moved toward the position of initial fixation at a constant speed. Targets moved away from the position of fixation only in one set of experiments designed to look in parallel at the effects of initial target position on the initiation of pursuit and the discharge of FPA neurons. The size of target step ranged from 1 to 18°, and the speed of target motion ranged from 5 to 40°/s. The initial fixation target was presented at the center of the screen in most trials, but it appeared 10° eccentric when we examined the velocity sensitivity or the eye-position sensitivity of the activity of pursuit-related neurons. In all pursuit trials, the target moved at constant speed for 300–1,000 ms and then stopped and remained stationary for 500–1,200 ms before disappearing. The fixation period at the end of each pursuit trial provided a way to control for any relationship between firing rate and eye position and also helped to maintain excellent pursuit during the prior target motion.

## Physiological procedures

Neuronal activity was recorded through tungsten microelectrodes (Frederick Haer) lowered into the periarcuate cortex using a hydraulic micromanipulator (Narishige MO-95). The electrodes typically had impedances of 1–2 MΩ at 1 kHz (BAK Electronics). The location of electrode penetrations was adjusted by an *X*-*Y* stage attached on the top of the cylinder. When we searched for pursuit-related neurons, the monkeys performed a block of pursuit trials (20°/s) and saccade trials (16°) in four to eight different directions. We also used electrical microstimulation to locate sites where we might find neurons related to pursuit. The stimulation was applied through the same electrode every half millimeter along each penetration. The stimulation consisted of a train of 0.2-ms cathodal pulses for 75 ms at 333 Hz. The intensity of current was 50 μA and was monitored by measuring the voltage across a 1-kΩ resistor placed in series with the electrode. Once we encountered pursuit-related multiunit activity or found a site where microstimulation evoked smooth eye movements, we attempted to isolate pursuit-related single neurons. The occurrence of each spike was detected using a commercial window discriminator (BAK Electronics) during the experiments. Since the goal of our study was to examine the activity of pursuit-related single neurons in a variety of behavioral conditions, we made more efforts to isolate single neurons that had sustained activity during pursuit, and less to record from other types of neurons including saccade-related burst neurons or fixation-related neurons. This sampling procedure certainly biased our sample of neurons to contain a higher proportion of pursuit-related neurons than actually exists in the periarcuate cortex.

## Data acquisition and analysis

Horizontal and vertical eye position signals were obtained directly from the eye coil electronics (CNC Engineering). To obtain signals related to eye velocity, the eye position voltage was passed through analog circuits that differentiated frequencies up to 25 Hz and rejected higher frequencies (−6 dB/octave). Analog data were digitized and sampled at 1 kHz. Logic pulses from the window discriminator were time-stamped with a resolution of 10 μs. All data were stored on a hard disk during experiments and were analyzed later on a UNIX workstation.

To analyze eye movements during pursuit, we reviewed traces of eye position and eye velocity of each trial on a video monitor, detected saccades visually, and marked them with a mouse-controlled cursor using an interactive computer program. The use of a manual marking procedure ensured that the entire saccade was marked. Portions of the eye velocity traces during saccades were not used for the subsequent analyses performed with Matlab (Mathworks). Thus the traces of average eye velocity in our figures are means that may have been computed from a different number of samples at different time points. To analyze eye movements during saccade trials, saccades were detected by an automatic algorithm. Net eye speed was computed after filtering horizontal and vertical eye velocity by applying a 29-point finite impulse response differentiator (−3 dB, 50 Hz) to the horizontal and vertical eye position data. The

onset of saccades was marked as 1 ms before the time when eye speed had exceeded 10°/s, and eye position had changed by more than 0.2°. The offset of saccades was marked as 1 ms after eye speed crossed 10°/s on the way back to zero. The automated analysis of saccade onset and offset was used only to indicate the time of saccades in saccade trials, and not to determine which parts of a trial would be excluded from further analysis in pursuit trials. We used the different techniques to detect saccades for different tasks so that we could analyze our data as accurately as possible given the constraints imposed by the saccades. When we used analog differentiation, the duration of the deflection in eye velocity associated with saccade was longer than that of saccade measured from eye position traces (see Fig. 1 of Lisberger 1998). This means that the time of saccade offset marked manually in pursuit trials was somewhat later than the time of actual saccade termination. Manual detection ensured that we removed the entire deflection before analyzing smooth eye velocity. The digital differentiation technique allowed us to identify saccade offset more accurately for saccade trials, when we were not measuring smooth eye velocity.

For further analysis, both eye movement and neuronal responses were aligned on the onset of target motion or the step of target position for all responses to identical target motions in the same block. To show the time course of neuronal activity in our figures, each occurrence of an action potential was summed across multiple trials and the result was convolved with a Gaussian filter ($\sigma = 10$ ms) (Richmond and Optican 1987) using a temporal resolution of 1 ms. All quantitative analyses, however, were based on the spike counts that were made from individual trials in specific time intervals relative to the target motion onset. Since the variation of pursuit latency is minimal for trained monkeys (Lisberger and Westbrook 1985), the results would not have been materially different if we had aligned analyses on the time of pursuit initiation. Details are provided at the relevant places in RESULTS.

The latency of pursuit and the neuronal activity were measured by using the receiver operating characteristic (ROC) analysis (Egan 1975; Green and Swets 1966) that has been used for the analysis of single neuron data (e.g., Bradley et al. 1987; Britten et al. 1992; Thompson et al. 1996). Eye velocity analysis was based on the component eye velocity along the axis of eye movements evoked by target motion along the preferred axis of the neuron under study. The axis was determined by linear regression of the eye velocity measured 180 ms after the onset of target motion in the preferred and opposite directions. Neuronal analysis was based on the spike density (see following text) obtained from each trial with a resolution of 1 ms. Before conducting the ROC analysis, the component eye velocity and the unit data were convolved in parallel with two functions to compare the results obtained with different filtering methods. Filters were a Gaussian function ($\sigma = 8$ ms) and a double exponential function that has been used for the analyses of cortical neuronal activity (Hanes et al. 1998; Hanes and Schall 1996; Thompson et al. 1996). The double exponential filter was originally designed to model the time courses of postsynaptic potentials and was described by

$$y=(1 - e^{-t/a})e^{-t/b} \quad (1)$$

where $a$ and $b$ determined the time constant for the growth and the decay phases, and were 1 and 20 ms, respectively.

The filtered data were averaged over 5-ms intervals for a 250-ms period starting from the onset of target motion. To construct the ROC curve for each 5-ms interval, we computed the “Hit rate” and the “False-Alarm rate” for the responses to target motion in the preferred pursuit direction and those in the opposite direction at each level of a criterion that was increased in steps of 1°/s (eye velocity) or 5 spikes/s (unit data). The areas under the ROC curves were then

plotted as a function of time and were fitted with the scaled Weibul distribution function (Hanes et al. 1998; Thompson et al. 1996) described by

$$y=p-(p-q)e^{(-t/r)^s} \quad (2)$$

where $p$ and $q$ define the minimal and maximal values of the curve, respectively. The parameters of $p$, $q$, $r$, and $s$ were computed using Matlab to find the best fit by a least-squares criterion. The coefficient of determination ($r^2$) of the fitted curves was typically approximately 0.9, and data with $r^2 \leq 0.7$ were excluded from further analyses. The analysis compared responses in the preferred and opposite direction for the neuron under study to estimate the onset of a directional response, which was taken as the time when the Weibul distribution curve crossed 0.75. The latency of both eye movements and neuronal activity were measured using each of the two different filters described above and were compared with those measured visually by experimenters.

Since both monkeys are currently being used for other experiments, we are unable to provide histological verification of recording sites.

## RESULTS

### Database and classification of neurons

Data were collected from three hemispheres of two monkeys. Table 1 summarizes the numbers of neurons examined in this study. Among 166 neurons tested, 148 (89%) were grouped into one of three categories. The majority of neurons (54%) showed sustained activity during pursuit in one or more directions. These cells typically showed little or no activity during saccades. The cells in the second large group (25%) displayed a burst of activity during saccades, but did not respond strongly during pursuit. The third group (10%) showed activity related to eye position in the orbit. The other 11% of the neurons showed activity related to fixation ($n$ = 5), pursuit termination ($n$ = 7), target offset ($n$ = 2), or other visual events ($n$ = 4).

Figure 1 plots time courses of the activity of the population for each of the three groups of neurons in pursuit and saccade trials. The population activity was computed by normalizing all the spike density profiles from each cell for the maximal value in the spike density curves for pursuit at 20°/s and saccades of 16° in each direction. Each response was aligned on the onset of either target motion (Fig. 1, *A*, *C*, and *E*), the target step (Fig. 1, *B*, *D*, and *F*), or the saccade (not shown), and averages of the normalized responses were computed in each group. In agreement with previous studies (Gottlieb et al. 1994;Tanaka and Fukushima 1998), the population of pursuit cells showed sustained activity during pursuit of target motion in the preferred direction (solid trace in Fig. 1*A*) and relatively little response during pursuit in the opposite direction (dashed trace in Fig. 1*A*). Importantly, pursuit neurons ceased firing at the end of the pursuit trial, when the target stopped moving. Pursuit neurons also had a trace of activity after the step of target position in saccade trials, because 10 pursuit neurons (12% of 83) showed a strong burst of activity during saccades of 16° (Fig. 1*B*). The preferred direction of the burst was the preferred pursuit direction for four neurons, the opposite direction for two neurons, and in both directions for four neurons.

Saccade cells displayed a burst of activity that started just after the target step in one direction (solid trace in Fig. 1*D*) and that peaked at the onset of the subsequent saccade (not shown). They showed relatively little activity for saccades in the opposite direction (dashed trace in Fig. 1*D*) and little or no modulation of firing during pursuit in either direction (Fig. 1*C*). Position neurons showed an increase in firing rate during pursuit in the preferred direction (solid trace in Fig. 1*E*) and for saccades in the preferred direction (Fig. 1*F*). However, they

differed from pursuit neurons by showing continued activity when the target stopped and the monkey maintained fixation at the eccentric location after the end of the ramp target motion. They also differed from saccade neurons in maintaining the increase in activity at the new eye position after saccades. Most position neurons (10 of 15) showed a weak burst of activity during saccades in the same ($n$ = 5) or opposite ($n$ = 5) direction as the eye position-related activity. Figure 1 does not include data from 11 neurons (7 pursuit, 3 saccade, and 1 position) that were not studied during the exact target motions used to conduct this analysis.

In this and the accompanying paper, we analyze the responses of the pursuit neurons identified by the screening procedure outlined in Fig. 1.

## Directionality of pursuit responses

Almost all pursuit neurons were directional, as in previous studies (Fukushima et al. 2000; Gottlieb et al. 1994; Tanaka and Fukushima 1998). The number of spikes during a 1,000-ms period of target motion in one direction was statistically different from that for target motion in the opposite direction for 86 of 90 neurons (2-tailed $t$-test, $P < 0.01$). The rasters in Fig. 2*A* show the activity of a typical pursuit neuron during tracking of target motion in the eight different directions indicated by the arrows on the left. The neuron had a modest resting discharge, showed a large increase in firing during upward pursuit, and was inhibited slightly during downward pursuit. To quantify the directional preference, we fitted a Gaussian function to a plot of the mean firing rates in a 600-ms interval that began 100 ms after the onset of target motion versus the direction of target motion (Fig. 2*B*). The fitted Gaussian was centered at 89.9° and had a value of σ of 49.6°, corresponding to a full-width at half-maximum (FWHM) of 116.8°. Figure 2*C* summarizes the tuning curves of all 52 neurons that were tested for pursuit in 8 different directions. The mean and SD of the tuning were computed after each individual tuning curve had been normalized for its peak value and shifted along the horizontal axis to align the centers. The values of σ of the fitted Gaussian functions ranged from 18.5 to 163.0°, and averaged 54.6 ± 23.5° (SD, $n$ = 52), which corresponds to a mean FWHM of 128.6 ± 55.4°.

There was no relationship between the preferred direction of pursuit neurons and the side of recording. In Fig. 2*D*, the direction of each vector indicates the preferred direction of a neuron derived from the Gaussian curve, and the length of each vector indicates the peak value of the Gaussian minus baseline firing rate measured 300 ms before target motion onset (e.g., horizontal dashed lines in Fig. 2, *B* and *C*). Two statistical tests supported the impression gained from inspection of Fig. 2*D* of a uniform distribution of preferred directions without any strong bias toward a certain direction, consistent with previous studies (Fukushima et al. 2000;Gottlieb et al. 1994;Tanaka and Fukushima 1998). Rayleigh's test did not reject the hypothesis that the preferred directions were uniformly distributed (mean vector length $r$ = 0.13, $n$ = 52, $P > 0.1$); the amplitudes of maximal modulation were not dependent on preferred directions (Mardia's linear-circular rank correlation coefficient $D_{52}$ = 0.037, $P > 0.1$).

## Latency of directional signals

To determine how to analyze latency without biasing the results, we first compared several different approaches to estimating the latency of neuronal and eye velocity responses. Figure 3*A* shows that the eye velocity estimates using the double-exponential filter (open symbols) tend to be delayed with respect to those using the Gaussian filter (filled symbols) and the unfiltered trace (obscured by the filled symbols). The ROC analysis yielded estimates of the time of divergence of the eye velocity traces for the two directions of target motion that were later for the double exponential filter (downward arrow) than the Gaussian filter (upward arrow). Figure 3*B* plots the cumulative sum of spikes starting from the onset of target motion for either direction. Again, the ROC analysis yielded a shorter latency for the Gaussian filter (upward arrow) than for the double-exponential filter (downward arrow). Figure 3*C* illustrates

the ROC analysis on which the latency estimates were based when the Gaussian filter was applied to data from this particular neuron. The Weibul function fitted to the areas under ROC curves for the measurements of eye velocity (filled symbols) reached the criterion value of 0.75 about 21 ms after that for the neuronal activity (open symbols). Note that this analysis is based on comparison of the eye movement and neuronal responses in opposite directions, and thus estimates the latency when the two responses are significantly directional, and not merely the time when the neuronal activity rises above baseline.

To test the validity of our measurements using different filters, we next compared the values derived from the ROC analysis with those measured by detecting visually the onset of directional responses in the average eye velocity and the cumulative spike counts. The data were included in our sample if the time courses of areas under the ROC curves were fitted by the Weibul function with $r^2 > 0.7$ in the analysis of Fig. 3*C*, and the fitted curves exceeded the criterion value of 0.75. Of the 86 neurons that were directional based on statistical comparison of firing during pursuit in the preferred and opposite directions (see the last section), the data from 64 (Gaussian filter) and 69 (double-exponential filter) neurons satisfied these criteria. Comparison of the latency estimated by the ROC analyses and the latency estimated by visual inspection of the traces confirmed the impression given in Fig. 3, *A* and *B*: the estimates from the double-exponential filter were a little too long, while those from the Gaussian filter agreed with the visual estimates: when latency measured objectively was plotted as a function of latency estimated visually, the points for the Gaussian filter (filled symbols, Fig. 3, *D* and *E*) fell close to the line of equality, while those for the double exponential filter (open symbols, Fig. 3, *D* and *E*) were consistently above the line. For eye movements, the use of the double-exponential and the Gaussian filters showed longer latency than visual estimation by 20.0 ± 7.6 ms and 4.8 ± 6.5 ms ($n = 90$), respectively. For the neuronal activity, the use of the double-exponential filter again showed longer latency than visual estimation by 11.1 ± 10.1 ms ($n = 69$), whereas the use of the Gaussian filter showed latencies that were closer and slightly shorter than those measured visually (−3.3 ± 10.5 ms, $n = 64$). The better agreement between the visual analysis and the estimates based on ROC analysis of Gaussian filtered data are expected, since the Gaussian filter is symmetrical and should not alter the latency of the data, while the double-exponential filter is noncausal and should introduce some delay to the filtered traces.

Finally, we compared neuronal and behavioral latency for each neuron using the ROC analysis based on the Gaussian filtered data, because this objective method seemed to agree best with our visual estimates of latency. Figure 3*F* plots neuronal latency as a function of pursuit latency for the 64 neurons that satisfied the criteria set out for admitting the ROC estimates based on the Gaussian filter. Of the 64 neurons, 37 (58%) plotted below the unity line, indicating that they showed directional modulation of firing rate that led the initiation of pursuit. However, only 12 (19%) showed directional modulation of firing rate that led pursuit by more than 25 ms (dashed oblique line). Thus a minority of neurons exhibited responses that could affect eye velocity before the mean latency of the smooth eye movements evoked by electrical stimulation in the FPA (Tanaka and Lisberger 2002). The median of the latency difference between firing rate and pursuit initiation was 8.5 ms, with firing rate leading pursuit.

### Sensitivity to eye velocity

In general, the firing rate of pursuit neurons increased as a function of pursuit eye speed in the preferred direction of the neuron. Figure 4*A* shows an example of eye and neuronal responses for target motion at five different speeds in the preferred direction. We measured the sensitivity to eye velocity from each individual trial in two different intervals. For the initiation of pursuit, both eye speed and neuronal firing rate were averaged over a 250-ms period starting 50 ms after target motion onset. For the maintenance of pursuit, the responses were measured during a 500-ms interval starting 400 ms after target motion onset. Each trial began with fixation at

10° eccentric location in the direction opposite to target motion so that we could examine the responses to different speeds as the eye crossed roughly straight-ahead gaze.

Both neurons illustrated in Fig. 4, *B* and *C*, showed higher firing rates during the initiation of pursuit (**X**) than for the maintenance of pursuit (●). For the neuron in Fig. 4*B*, the regression lines have slopes of 4.74 and 1.71 spikes/s per deg/s with correlation coefficients of 0.77 and 0.81 for the initiation and the maintenance intervals, respectively. In contrast, the response of the neuron in Fig. 4*C* showed a relationship to eye speed during pursuit initiation (slope 1.73, $r = 0.35$), but not during the maintenance of pursuit (slope 0.18, $r = 0.12$). Still, the firing of this neuron for pursuit of all target speeds was well above the baseline firing measured from the 300-ms interval before target motion onset (horizontal dashed line), and its responses were strongly direction selective during both the initiation and the maintenance of pursuit.

Figure 5 summarizes the sensitivity to eye speed in the preferred direction for 43 pursuit neurons that were deemed to be directional by the analysis presented in the previous section. This sample includes 25 neurons that were studied during 5 different target velocities according to the protocol described for Fig. 4 (solid lines in Fig. 5, *A* and *B*, and filled symbols in Fig. 5*C*), and 18 neurons that were tested only for target motion at 5, 10, and 20°/s (dashed lines in Fig. 5, *A* and *B*, and open symbols in Fig. 5*C*). For the latter neurons, the fixation target appeared at the center of the screen and target motion began 1, 2, and 4° eccentric for the three target speeds. As will be seen below, the details of the target motion and the number of target speeds did not affect the distribution of neural responses.

For both the initiation (Fig. 5*A*) and maintenance (Fig. 5*B*) analysis intervals, there was a wide range of regression lines and a trend toward higher firing rates and steeper regression lines for the initiation versus maintenance intervals. Comparison of the regression slopes for the different analysis intervals in individual neurons reveals that most neurons plot below the unity line in Fig. 5*C* and therefore had higher values of sensitivity during the initiation interval. The values of regression slopes ranged from −6.93 to 9.36 spikes/s per deg/s with the median of 2.84 for the initiation of pursuit, and those for the maintenance of pursuit ranged from −0.89 to 3.40 spikes/s per deg/s (median, 0.96). These values were statistically different (Wilcoxon signed-rank test, $P < 0.001$). Note that some neurons plotted with sensitivities to eye velocity that were near zero for one or both intervals. There neurons were strongly directional, showing firing rates that were above baseline during pursuit in the preferred direction, but their firing rate did not depend on eye speed over the range we tested. The sensitivity to eye velocity did not depend on whether the directional modulation of neuronal activity preceded the initiation of pursuit by greater than (triangles in Fig. 5*C*) or less than (circles in Fig. 5*C*) 15 ms.

## Parallel effects of initial target position on eye acceleration and neural responses during the initiation of pursuit

Eye acceleration during the initiation of pursuit for a step of target velocity depends on the initial retinal position of the moving images (Lisberger and Westbrook 1985). To look for the neural basis for this feature of pursuit, we recorded the activity of FPA pursuit neurons during pursuit initiation for targets that started at different locations in the visual field. As before, animals tracked step-ramp target motion, but we kept the speed of the ramp constant while varying the size of the target step to place the moving images at different locations along the axis of target motion.

Figure 6, *A* and *B*, shows the time courses of pursuit initiation up to the time of the first tracking saccades in most trials, for rightward target motion that started in the left or right visual field and moved toward (*A*) or away from (*B*) the position of initial fixation. Presaccadic eye acceleration was degraded as the eccentricity of target images increased for both the target moving toward (*A*) and away from (*B*) the position of initial fixation: acceleration was highest

for targets close to the position of fixation (red traces) and decreased as they appeared further and further from the position of fixation (blue, green, and black traces, respectively). Figure 6, *C—E*, show neural responses of three typical neurons to illustrate that they underwent parallel decreases in response size. Each trace plots the time course of spike density filtered with a Gaussian with a σ of 10 ms. When the target started close to the position of initial fixation and the presaccadic initiation of pursuit was strong (red and blue traces), all three neurons gave the strongest early responses. When the target started more eccentric and the presaccadic initiation of pursuit was weaker (green and black traces), the early response of these three pursuit neurons was similarly reduced. Two features of these data are worth noting. First, the firing rates converge by the end of the 300-ms interval shown in Fig. 6, *C–E*, when pursuit eye velocity also had converged to a value near target velocity. Second, the decreases in response amplitude as a function of initial image position are generally not associated with an increase in latency, making it difficult to attribute the reduced firing to starting the target outside the visual receptive field of the neuron. If the changes in response amplitude were due to the size of the visual receptive field, then changing initial target position by 6° would increase response latency by 300 ms for target motion at 20°/s. However, the change in latency was absent (Fig. 6*C*) or small relative to this prediction (Fig. 6, *D* and *E*).

To analyze the correlation between eye acceleration and the neuronal activity during the initiation of pursuit for target motion at different retinal locations, we first measured eye acceleration from individual traces of eye speed for the period 121–180 ms after target motion onset and firing rate in the interval from 91 to 180 ms after target motion onset. Very few trials had saccades with latencies shorter than 190 ms, and these were excluded from the analysis. As reported previously (Lisberger 1998; Lisberger and Westbrook 1985), initial eye acceleration was greatest when the target started to move near the position of fixation, and declined as a function of eccentricity of initial target position, both during recordings from individual neurons (Fig. 7*A*) and for the average across all 23 recordings made for this experiment (Fig. 7*B*). The magnitudes of neuronal responses showed a similar property, as illustrated in Fig. 7*C* for the 3 neurons shown in Fig. 6, and in Fig. 7*D* for the average across all 23 neural recordings. Neuronal responses were largest when the target started close to the position of initial fixation and, like eye acceleration, declined as a function of eccentricity.

There was a strong correlation between the magnitude of the initial eye acceleration and the firing rate response associated with the corresponding initial target position. For the three cells used to construct Fig. 7*C*, the correlation coefficients were 0.89, 0.92, and 0.89. We found statistically significant correlations ($P < 0.05$) between eye acceleration and the neuronal activity for 18 of the 23 neurons tested in this experiment (78%). The median and mean of the correlation coefficients were 0.85 and 0.77 ± 0.20 ($n = 23$). The correlation coefficient of the means of normalized responses was 0.93, and was statistically significant ($P < 0.01$). Thus eye acceleration during the initiation of pursuit was highly correlated to the activity of individual neurons as well as to the average response of the population of FPA pursuit neurons.

## Absence of responses to retinal position error in most pursuit neurons

We now ask whether pursuit neurons in the FPA encode small position errors during pursuit, as do many neurons in the rostral pole of the superior colliculus (Krauzlis et al. 1997, 2000). We do this with two separate experiments asking whether these neurons fire in relation to the retinal position of target images *1*) before saccades to a stationary target and *2*) during the initiation and the maintenance of pursuit.

**RESPONSES TO TARGET STEPS DURING FIXATION—**First, we examined the responses to target steps that elicited saccades with a variety of amplitudes (0.5, 1, 2, 4, and 16°) along the preferred axis of pursuit for the neuron under study. For 22 neurons, the central

fixation target disappeared at the onset of the peripheral target; for 13 neurons, we used an overlap task where the fixation target remained on for 300 ms after the onset of peripheral target to lengthen the latency of saccades. In both tasks, the monkeys were required to keep eye position within 1° of the fixation target as long as it was visible.

Figure 8 shows the responses to target steps in the overlap task for a single pursuit neuron that had sustained activity during downward pursuit (Fig. 8*A*, *left column*) and was inhibited during upward pursuit (Fig. 8*A*, *right column*). In the interval between the onset of the eccentric target (vertical solid lines) and the offset of the fixation spot (vertical dashed lines), this neuron showed a slight decrease in firing for target steps in the preferred pursuit direction (Fig. 8*B*, *left column*), and a slight increase for steps in the opposite direction (Fig. 8*B*, *right column*). In the interval surrounding the onset of the saccade (filled circles in rasters), the firing of this neuron was unchanged or slightly suppressed for saccades in the preferred pursuit direction (*left column*) and increased for saccades in the opposite direction (*right column*). The responses to target steps were measured from four intervals as follows; *1*) interval from 90 to 169 ms after target onset (visual response); *2*) interval from 180 ms after target onset to 50 ms before saccade onset (delay); *3*) interval from 40 ms before to 39 ms after saccade onset (saccade), and *4*) 80-ms interval after saccade offset (postsaccade). We were able to measure the delay activity only for the data obtained using the overlap task, and only for trials that had saccade latency >310 ms so that the duration of the delay period would be at least 80 ms.

*Cells 1* and *2* in Fig. 9 illustrate typical examples of responses found in 31 of the 35 neurons tested during steps of target position and saccades: no modulation or only a small modulation in activity in each of the analysis intervals. In both neurons, the responses during pursuit in the preferred direction (filled circles) were considerably larger than those during the saccade task (open symbols). Responses during pursuit in the preferred direction (filled circles) were computed as the maximum of the mean firing rate measured in sequential 80-ms bins from 80 to 600 ms after target motion onset and were plotted as a function of the mean retinal image position in the previous 80 ms. Data for pursuit in the opposite direction (filled diamond) were measured for the same task intervals as those used for pursuit in the preferred direction. We chose the binwidth on the assumption that the delay of visual responses in the FPA is about 80 ms. Since the neuronal responses were maximal during the initiation of pursuit and immediately before the step-ramp target crossed the position of initial fixation (180 and 122 ms after target motion onset for the *cells 1* and *2*), the retinal image position during pursuit was opposite to the direction of pursuit, so that the point for pursuit in the preferred direction (filled circle) plots to the left of that for pursuit in the opposite direction (filled diamond). Since the cell in the *middle column* (*cell 2*) was not studied in the overlap paradigm, we were unable to measure the delay period activity.

*Cell 3* in Fig. 9 illustrates data for one of the four neurons (11% of 35), that showed greater activity during large saccades (16°) than during pursuit. The neuron showed weak visual responses (*C*), strong delay period activity (*E*), and a presaccadic burst of activity (*H*) for saccades in the preferred pursuit direction, which was toward the visual field contralateral to the site of the recording. The movement field was open-ended within the range we tested. Electrical microstimulation applied at the sites of the four neurons that showed strong saccade-related activity evoked either no eye movements (1 site) or saccades (3 sites including the site of *cell 3*), rather than smooth continuous eye movements that were often evoked by stimulation in the FPA.

The *right column* of Fig. 9 summarizes the responses of the 31 neurons that were like *cells 1* and *2*: 11 of these neurons were studied with the overlap paradigm and contributed to the analysis of the delay period activity. To give a sense of the activity during saccades relative to that during pursuit, the responses of each neuron were normalized for the maximal activity

during pursuit before the averages were computed. Pursuit neurons had only a weak visual response to steps of target position and little or no response during the delay interval, or during or after saccades. The peak of the weak visual responses occurred for steps of target position in the direction opposite to the preferred pursuit direction, and the magnitude of the visual response was much smaller than the maximal pursuit response (unity on the ordinate).

**RELATION TO RETINAL IMAGE POSITION DURING PURSUIT—**We next examined whether the firing of pursuit neurons during the initiation and the maintenance of pursuit was related strongly to retinal image position. Our approach was to plot firing rate as a function of image position 80 ms earlier and see whether this provided any consistent accounting of the firing rate during pursuit in the preferred and the opposite direction (Fig. 10). Firing rate was analyzed for the interval from 120 to 560 ms after target motion onset in 1-ms time steps. Each symbol in the graphs was obtained by averaging firing rate over an 80-ms interval centered on each time step and averaging retinal image position over the preceding 80 ms. Thus the measurement intervals for the neuronal activity ranged from 80–159 to 521–600 ms after target motion onset, and those for image position ranged from 0–79 to 441–520 ms after target motion onset.

Consider first the example neuron summarized by Fig. 10*A*. For motion in the preferred direction, the target stepped 4° up and then moved downward at 20°/s. In the first 80 ms, the eyes did not move, so that the retinal image position of the moving target averaged −3.2°: as a result the first point for pursuit in the preferred direction in Fig. 10*A* (right and upward pointing arrow) plots at an image position of −3.2° and a firing rate of about 45 spikes/s. As pursuit was initiated, the retinal image position covered both positive and negative values, but firing rate remained high. The mirror image situation obtained for target motion in the opposite direction. The first point (left and downward pointing arrow) plots at an image position of + 3.2° and a firing rate below the baseline firing measured from 300 ms before target motion onset (horizontal dashed line). As pursuit continued, the retinal image position covered retinal image positions that overlapped those during pursuit in the preferred direction, but the firing rate remained consistently low. The same general finding can be seen for the individual neurons plotted in Fig. 10, *B* and *C*, and for the average of all 35 neurons tested in this experiment (Fig. 10*D*). The activity during pursuit in the preferred direction (filled symbols) was consistently greater than that during pursuit in the opposite direction (open symbols) for any given retinal image position of the target. Further, neither curve gives any evidence for a strong relationship between firing rate and retinal image position during pursuit in either the preferred or the opposite direction.

## Sensitivity to eye position in the orbit

To examine whether eye position in the orbit affected the response of pursuit neurons, we provided the same step-ramp target motion starting with the fixation target located at the center of the screen or 10° eccentric in both directions along the axis of target motion. The pursuit stimulus consisted of a ramp speed of 20°/s in the preferred direction and a step amplitude of 3° in the opposite direction, and was followed by a second fixation at the final position achieved by the ramp motion. The duration of target motion was 900 ms for the cells with horizontal or oblique preferred directions, but was 500 ms for the cells with vertical preferred direction because of the limitation of the size of the screen.

Two example neurons were used to create the rasters and spike density functions (solid traces) shown in Fig. 11. In all panels of this figure, the target moved during the interval between the two vertical lines. The activity of the neuron shown in the *top row* was subtly affected by the orbital eye position traversed by pursuit. The initial firing rate during pursuit increased slightly as the orbital position of pursuit changed from 10° in the nonpreferred direction (*left raster*)

to straight-ahead gaze (*middle raster*) to 10° in the preferred direction (*right raster*). The effect of eye position cannot be seen during either the first or second fixation period (i.e., before and after the motion period), suggesting that the subtle effect on the early part of the response represents an effect on the gain of the response, rather than addition of an eye position signal. The activity of this neuron was typical of 11 of 12 neurons tested in this paradigm. The neuron illustrated in the *bottom row* of rasters showed strong eye position effects. For this neuron the effect of orbital position was present in the initial and the sustained response during pursuit, but again was not evident in either fixation interval.

We examined the effect of eye position on responses during pursuit for 12 pursuit neurons. For each neuron, we measured the mean firing rate for each initial target position during: the 300 ms immediately before target motion onset (1st fixation interval); the interval from 100 to 499 ms after target motion onset (pursuit interval); and the interval from 300 to 599 ms after target motion offset (2nd fixation interval). Figure 12*A* plots the data from all 12 neurons we tested, with the data from Fig. 11 plotted as filled symbols connected by bold lines. With the exception of the neuron in the *bottom row* of Fig. 11, the effects of orbital position on the mean response during pursuit were subtle. Correlation coefficients were > 0.5 in only two, four, and one neurons for the first fixation, pursuit, and second fixation intervals, respectively. Only four neurons showed regression slopes > 1.0 spikes/s per deg during pursuit (arrows in Fig. 12*A*). The slopes of the regression lines averaged −0.07 ± 0.47, 0.71 ± 1.30, and −0.17 ± 0.39 spikes/s per deg and had medians of 0.04, 0.57, and −0.19 spikes/s per deg for the first fixation, pursuit, and the second fixation intervals, respectively. Thus the effects were not strong, although they were statistically significant ($P < 0.05$) for three, seven, and two neurons in the three measurement intervals. For the population, the one-way factorial ANOVA failed to reveal significant eye position effects for any of the three analysis intervals ($P > 0.5$).

Effects were clearer when we examined the eye acceleration and neuronal firing rate at the initiation of pursuit for different initial fixation locations. Eye acceleration was measured from 121 to 200 ms after target motion, and neuronal firing rate was measured from 91 to 200 ms after target motion onset for each of the three initial fixation locations. The data for the fixation locations at ±10° were normalized for the responses in trials with central fixation by computing the ratio of the responses to eccentric versus central initial positions. Inspection of Fig. 12*B* suggests that the neuronal response was higher for an initial target position of + 10° (filled symbols) than for −10° (open symbols) for 7 of the 11 neurons we were able to include in this analysis (1 neuron did not fire until after the analysis intervals). Regression analysis showed no significant correlation between neuronal response and eye acceleration ($r = 0.22$, $n = 22$, $P > 0.1$). However, a repeated-measures ANOVA showed significant effects of initial target position on the neuronal firing rate ($P < 0.01$), but not on the initial eye acceleration ($P > 0.05$).

## DISCUSSION

The goal of our study was to extend knowledge of the responses of pursuit neurons in the FPA during tracking paradigms designed to help us understand better how the FPA fits into the overall circuitry of the pursuit system. Pursuit neurons were found near the arcuate sulcus, and had similar response properties to those reported previously (Fukushima et al. 2000; Gottlieb et al. 1994; Tanaka and Fukushima 1998). They were active during the initiation and the maintenance of pursuit in one or more directions, and only a few (12%) showed strong responses during saccades. More than one-half of the neurons (58%) showed directional responses that started before the initiation of pursuit, while electrical microstimulation applied at or near the recording sites often evoked ipsiversive smooth eye movements (Tanaka and Lisberger 2002). Thus responses in the FPA would be suitable to contribute to both the initiation and maintenance of pursuit.

During pursuit of different target velocities in the preferred direction, the sensitivity to eye velocity was greater during the initiation than during the maintenance of pursuit for most neurons, while the estimates of the latter were similar to those reported previously (Fukushima et al. 2000; Gottlieb et al. 1994). The higher sensitivity during the initiation of pursuit agrees with prior conclusions that neurons in the FPA carry visual motion signals and eye motion signals (Fukushima et al. 2000; Tanaka and Fukushima 1998). The visual motion signals would be large during the initiation of pursuit but minimal during the maintenance of pursuit, while eye velocity signals would cause the responsiveness during the maintenance of pursuit. Although we were unable to provide histological verification of the location of pursuit neurons, the similarity of the response properties argues that the neurons we examined in this study were the same population as those analyzed in the previous studies. Given the response properties of the pursuit neurons, it seems likely that their loss explains why lesions in the arcuate cortex cause pursuit deficits in both humans (Morrow and Sharpe 1990) and monkeys (Keating et al. 1991, 1993; Lynch 1987; MacAvoy et al. 1991; Shi et al. 1998).

### FPA is distinct from saccadic frontal eye fields

Until recently, the superior colliculus and FEFs were thought to be involved selectively in the generation of saccadic eye movements. However, recent studies have documented the existence of the FPA, which is part of the FEF, and clearly plays a role in pursuit. In parallel, a different line of analysis has raised the possibility that the rostral pole of the superior colliculus plays a role in pursuit. The rostral superior colliculus contains neurons that discharge during pursuit toward the contralateral side (Krauzlis et al. 1997, 2000) and that appear to be related to the retinal position error of target images. The same neurons also are active during the preparation as well as the execution of small saccades, indicating that they are a rostral extension of the buildup neurons recorded in caudal superior colliculus (Munoz and Wurtz 1995), active for targets that appear close to the fovea (Krauzlis et al. 1997, 2000). Thus it is probably correct to think of the rostral pole of the colliculus as a natural extension of the remainder of the colliculus, and of the full extent of the colliculus as a unified structure that provides commands in terms of retinal image position. One of the goals of the present study was to determine whether the FPA should be thought of in similar terms, as the foveal representation of the FEF that processes information related to retinal position error.

Our data are not consistent with the idea that the FPA is a foveal extension of the saccadic FEF. Most FPA pursuit neurons (~90%) respond only slightly to the appearance of a peripheral target, and they show little or no modulation of firing rate during the preparation or execution of saccades. The magnitudes of visual responses to the stationary target, when present, were consistently smaller than those measured from pursuit trials in which the target moved toward the position of initial fixation and in the preferred pursuit direction. Further, we did not find a substantial relationship between FPA firing rate and retinal image position during either the initiation or maintenance of pursuit. Instead, the activity during pursuit was consistently greater for target motion in the preferred direction than in the opposite direction at any given retinal location of the target images. We therefore conclude that the pursuit-related activity in the FPA is related to the direction and speed of pursuit, and that it provides the pursuit system with qualitatively different information than do the retinal position error signals that are found in the rostral superior colliculus and would likely exist in the saccadic FEF.

Our observations are consistent with the recent proposals that the arcuate cortex contains functionally separate oculomotor regions related to saccadic and pursuit eye movements (Gottlieb et al. 1993, 1994; Lynch 1987; Petit and Haxby 1999; Tanaka and Fukushima 1998). The functional segregation of the two eye movement systems at the level of the arcuate cortex is consistent with the anatomical separation of the two areas in *Cebus* monkeys (Tian and Lynch 1996, 1997) and with the observation that the FPA of *Cebus* monkeys sends only

a sparse projection to the superior colliculus without topographic organization (Yan et al. 1999, 2001b). Further evidence for functional specialization in the oculomotor frontal cortex is provided by the report that the prearcuate cortex near the principal sulcus of monkeys contains cells that are exclusively active during vergence eye movements (Gamlin and Yoon 2000). However, the representation of different kinds of eye movements may also overlap: some areas in and near the arcuate sulcus exhibit some degree of overlap of vergence signals with both saccade signals (Ferrania et al. 2000) and pursuit signals (Fukushima et al. 2001). One issue for further research will be the functional basis of overlapping representations for different kinds of eye movements in the frontal cortex.

### Effects of orbital eye position on the activity of FPA neurons

The effect of eye position on neuronal activity is a common finding in the dorsal visual pathways and has been found in areas V3A (Galletti and Battaglini 1989), V6 (Galletti et al. 1995; Nakamura et al. 1999), LIP/7A (Andersen et al. 1990; Bremmer et al. 1997a), and MT/MST (Bremmer et al. 1997b). In many of the examples where eye position affects the firing of cortical neurons, the interaction with other signals is multiplicative rather than additive. We also found a few FPA neurons that showed a similar effect of eye position: as the orbital position traversed during pursuit was shifted in the preferred direction for pursuit, increased response gain caused greater neuronal activity during pursuit only. The modulation, however, was modest on the population level and was statistically significant only during the initiation of pursuit and not during pursuit maintenance. If the responses of FPA neurons are inherited from MT and MST, the modest eye position effect might be expected if the modulatory effects of eye position on the visual motion-sensitive neurons in MT and MST are balanced out at the population level (Bremmer et al. 1997b). The functional significance of the eye position effects we observed in the FPA is unclear at this time.

### Possible relations of the FPA neuronal activity to features of pursuit behavior

It has been known for some time that eye acceleration during the initiation of pursuit for a step of target velocity depends on the position of the target images in the visual field (Lisberger and Westbrook 1985). Initially, this effect was assumed to result from a change in the strength of the visual motion signals as a function of image eccentricity. However, it has been shown recently that the effect of the initial position of the moving images on pursuit initiation actually results from modulation of the gain of visual-motor conversion for image motion signals that are equally strong at all eccentricities (Lisberger 1998). In the present paper, we report that the activity of neurons in the FPA varies in parallel with the initial eye acceleration of pursuit as the position of the moving images used to initiate pursuit is varied. One interpretation of this result is that the FPA is downstream from the site where the gain is modulated, so that the firing rate of FPA neurons is related to the motor output rather than the visual input. Another interpretation is that the firing in the FPA controls the gain of visual-motor processing. We favor the latter interpretation because altering the output of the FPA with electrical micro-stimulation controls the gain of visual-motor processing (Tanaka and Lisberger 2001, 2002). However, this interpretation leaves open the question of why the initial response of FPA neurons depends on the position of the moving images if the strength of the signal emanating from visual motion areas does not.

Recently we have reported that the well-trained monkeys generate smooth eye movements in response to sudden appearance of a stationary, eccentric “cue,” if the cue appears in the temporal gap between the offset of the fixation spot and the appearance of a moving target (Tanaka and Lisberger 2000). The direction of the cue-evoked smooth eye movements was always away from the visual stimulus. The size of the responses was maximal for stimulus locations about 5° from the position of initial fixation. The latency of the cue-evoked smooth eye movements was slightly longer than that of pursuit, suggesting that the cue-evoked smooth

eye movements arise from pursuit pathways that run in parallel to those from the parietal visual motion areas to the pontine nuclei (Tanaka and Lisberger 2000). Further, the stationary cue had a separate effect that caused enhancement of the pursuit response to subsequent stimuli.

The responses of pursuit neurons in the FPA seem appropriate to mediate both of the effects of a stationary cue. Our data show that pursuit neurons in the FPA respond weakly to the appearance of a stationary target, giving the largest response when the target is about 4° eccentric in the direction opposite to the preferred pursuit directions of the neurons under study. Since one effect of FPA stimulation is to drive smooth eye movement, the increase in firing selectively for stimuli in the nonpreferred direction for pursuit would cause the cue-evoked smooth eye movements observed by Tanaka and Lisberger (2000), in the opposite, preferred direction. Since a second effect of FPA stimulation is to enhance the response to concurrent target motion (Tanaka and Lisberger 2001, 2002), the cue-evoked response of FPA neurons could also be responsible for the increased gain of the response to subsequent target motion reported by Tanaka and Lisberger (2000).

## Acknowledgements

We thank S. Tokiyama and G. Musacchia for technical assistance, K. MacLeod and L. Montgomery for surgical assistance, M. Meneses for animal care, S. Ruffner for software support, D. Kleinhesselink for network management, K. McGary for electronics, L. Bocskai for construction of mechanical devices, and N. Molyneaux for administrative assistance.

This study was supported by the Howard Hughes Medical Institute and by National Institute of Neurological Disorders and Stroke Grant P01-NS-34835.

## REFERENCES

Andersen RA, Bracewell RM, Barash S, Gnadt JW, Fogassi L. Eye position effects on visual, memory, and saccade-related activity in areas LIP and 7a of macaque. J Neurosci 1990;10:1176–1196. [PubMed: 2329374]

Basso MA, Krauzlis RJ, Wurtz RH. Activation and inactivation of rostral superior colliculus neurons during smooth-pursuit eye movements in monkeys. J Neurophysiol 2000;84:892–908. [PubMed: 10938315]

Bradley A, Skottun BC, Ohzawa I, Sclar G, Freeman RD. Visual orientation and spatial frequency discrimination: a comparison of single neurons and behavior. J Neurophysiol 1987;57:755–772. [PubMed: 3559700]

Bremmer F, Distler C, Hoffmann K-P. Eye position effects in monkey cortex. II. Pursuit- and fixation-related activity in posterior parietal areas LIP and 7A. J Neurophysiol 1997a;77:962–977. [PubMed: 9065861]

Bremmer F, Ilg UJ, Distler C, Hoffmann K-P. Eye position effects in monkey cortex. I. Visual and pursuit-related activity in extrastriate areas MT and MST. J Neurophysiol 1997b;77:944–961. [PubMed: 9065860]

Britten KH, Shadlen MN, Newsome WT, Movshon JA. The analysis of visual motion: a comparison of neuronal and psychophysical performance. J Neurosci 1992;12:4745–4765. [PubMed: 1464765]

Cui DM, Yan YJ, Lynch JC. Basal ganglia circuits related to visual pursuit in monkey. Soc Neurosci Abstr 2000;26:641.11.

Cui DM, Yan YJ, Lynch JC. Organization of projections from the frontal pursuit area to the putamen in *Cebus* monkeys. Soc Neurosci Abstr 2001;27:404.1.

Eckmiller R. Neural control of pursuit eye movements. Physiol Rev 1987;67:797–857. [PubMed: 3299410]

Egan, JP. Signal Detection Theory and ROC Analysis. New York: Academic; 1975.

Ferraina S, Paré M, Wurtz RH. Disparity sensitivity of frontal eye field neurons. J Neurophysiol 2000;83:625–629. [PubMed: 10634901]

Fuchs AF, Robinson DA. A method for measuring horizontal and vertical eye movement chronically in the monkey. J Appl Physiol 1966;21:1068–1070. [PubMed: 4958032]

Fukushima K, Sato T, Fukushima J, Shinmei Y, Kaneko CR. Activity of smooth pursuit-related neurons in the monkey periarcuate cortex during pursuit and passive whole-body rotation. J Neurophysiol 2000;83:563–587. [PubMed: 10634896]

Fukushima K, Yamanobe T, Shinmei Y, Fukushima J, Kurkin S, Peterson BW. Representation of smooth gaze movements in 3-D space by Frontal cortex in monkeys. Soc Neurosci Abstr 2001;27:404.8.

Galletti C, Battaglini PP. Gaze-dependent visual neurons in area V3A of monkey prestriate cortex. J Neurosci 1989;9:1112–1125. [PubMed: 2703870]

Galletti C, Battaglini PP, Fattori P. Eye position influence on the parieto-occipital area PO (V6) of the macaque monkey. Eur J Neurosci 1995;7:2486–2501. [PubMed: 8845954]

Gamlin PD, Yoon K. An area for vergence eye movement in primate frontal cortex. Nature 2000;407:1003–1007. [PubMed: 11069179]

Gottlieb JP, Bruce CJ, Macavoy MG. Smooth eye movements elicited by microstimulation in the primate frontal eye field. J Neurophysiol 1993;69:786–799. [PubMed: 8385195]

Gottlieb JP, Macavoy MG, Bruce CJ. Neural responses related to smooth-pursuit eye movements and their correspondence with electrically elicited smooth eye movements in the primate frontal eye field. J Neurophysiol 1994;72:1634–1653. [PubMed: 7823092]

Green, DM.; Swets, JA. Signal Detection Theory and Psychophysics. New York: Wiley; 1966.

Hanes DP, Patterson WF II, Schall JD. Role of frontal eye fields in countermanding saccades: visual, movement, and fixation activity. J Neurophysiol 1998;79:817–834. [PubMed: 9463444]

Hanes DP, Schall JD. Neural control of voluntary movement initiation. Science 1996;274:427–430. [PubMed: 8832893]

Huerta MF, Krubitzer LA, Kaas JH. Frontal eye field as defined by intracortical microstimulation in squirrel monkeys, owl monkeys, and macaque monkeys. II. Cortical connections. J Comp Neurol 1987;265:332–361. [PubMed: 2447132]

Keating EG. Frontal eye field lesions impair predictive and visually-guided pursuit eye movements. Exp Brain Res 1991;86:311–323. [PubMed: 1756806]

Keating EG. Lesions of the frontal eye field impair pursuit eye movements, but preserve the predictions driving them. Behav Brain Res 1993;53:91–104. [PubMed: 8466669]

Keller EL, Heinen SJ. Generation of smooth-pursuit eye movements: neuronal mechanisms and pathways. Neurosci Res 1991;11:79–107. [PubMed: 1656345]

Krauzlis RJ, Basso MA, Wurtz RH. Shared motor error for multiple eye movements. Science 1997;276:1693–1695. [PubMed: 9180078]

Krauzlis RJ, Basso MA, Wurtz RH. Discharge properties of neurons in the rostral superior colliculus of the monkey during smooth-pursuit eye movements. J Neurophysiol 2000;84:876–891. [PubMed: 10938314]

Leigh, RJ.; Zee, DS. The Neurobiology of Eye Movements. Vol. 2nd ed.. Philadelphia, PA: F.A. Davis; 1991.

Lisberger SG. Postsaccadic enhancement of initiation of smooth pursuit eye movements in monkeys. J Neurophysiol 1998;79:1918–1930. [PubMed: 9535958]

Lisberger SG, Ferrera Vp. Vector averaging for smooth pursuit eye movements initiated by two moving targets in monkeys. J Neurosci 1997;17:7490–7502. [PubMed: 9295395]

Lisberger SG, Morris EJ, Tychsen L. Visual motion processing and sensory-motor integration for smooth pursuit eye movements. Annu Rev Neurosci 1987;10:97–129. [PubMed: 3551767]

Lisberger SG, Westbrook LE. Properties of visual inputs that initiate horizontal smooth pursuit eye movements in monkeys. J Neurosci 1985;5:1662–1673. [PubMed: 4009252]

Lynch JC. Frontal eye field lesions in monkeys disrupt visual pursuit. Exp Brain Res 1987;68:437–441. [PubMed: 3691715]

Macavoy MG, Gottlieb JP, Bruce CJ. Smooth-pursuit eye movement representation in the primate frontal eye field. Cereb Cortex 1991;1:95–102. [PubMed: 1822728]

Morrow MJ, Sharpe JA. Cerebral hemispheric localization of smooth pursuit asymmetry. Neurology 1990;40:284–292. [PubMed: 2300251]

Munoz DP, Wurtz RH. Saccade-related activity in monkey superior colliculus. I. Characteristics of burst and buildup cells. J Neurophysiol 1995;73:2313–2333. [PubMed: 7666141]

Nakamura K, Chung HH, Graziano MS, Gross CG. Dynamic representation of eye position in the parieto-occipital sulcus. J Neurophysiol 1999;81:2374–2385. [PubMed: 10322073]

Petit L, Haxby JV. Functional anatomy of pursuit eye movements in humans as revealed by fMRI. J Neurophysiol 1999;82:463–471. [PubMed: 10400972]

Rashbass C. The relationships between saccadic and smooth tracking eye movements. J Physiol (Lond) 1961;159:326–338. [PubMed: 14490422]

Richmond BJ, Optican LM. Temporal encoding of two-dimensional patterns by single units in primate inferior temporal cortex. II. Quantification of response waveform. J Neurophysiol 1987;57:147–161. [PubMed: 3559669]

Schwartz JD, Lisberger SG. Initial tracking conditions modulate the gain of visuo motor transmission for smooth pursuit eye movements in monkeys. Vis Neurosci 1994;11:411–424. [PubMed: 8038118]

Shi D, Friedman HR, Bruce CJ. Deficits in smooth-pursuit eye movements after muscimol inactivation within the primate's frontal eye field. J Neurophysiol 1998;80:458–464. [PubMed: 9658064]

Stanton GB, Bruce CJ, Goldberg ME. Topography of projections to posterior cortical areas from the macaque frontal eye fields. J Comp Neurol 1995;353:291–305. [PubMed: 7745137]

Tanaka M, Fukushima K. Neuronal responses related to smooth pursuit eye movements in the periarcuate cortical area of monkeys. J Neurophysiol 1998;80:28–47. [PubMed: 9658026]

Tanaka M, Lisberger SG. Context-dependent smooth eye movements evoked by stationary visual stimuli in trained monkeys. J Neurophysiol 2000;84:1748–1762. [PubMed: 11024067]

Tanaka M, Lisberger SG. Regulation of the gain of visually-guided smooth pursuit eye movements by frontal cortex. Nature 2001;409:191–194. [PubMed: 11196642]

Tanaka M, Lisberger SG. Enhancement of multiple components of pursuit eye movement by microstimulation in the arcuate frontal pursuit area in monkeys. J Neurophysiol 2002;87:802–818. [PubMed: 11826048]

Thompson KG, Hanes DP, Bichot NP, Schall JD. Perceptual and motor processing stages identified in the activity of macaque frontal eye field neurons during visual search. J Neurophysiol 1996;76:4040–4055. [PubMed: 8985899]

Tian JR, Lynch JC. Functionally defined smooth and saccadic eye movement subregions in the frontal eye field of *Cebus* monkeys. J Neurophysiol 1996a;76:2740–2753. [PubMed: 8899642]

Tian JR, Lynch JC. Corticocortical input to the smooth and saccadic eye movement subregions of the frontal eye field in *Cebus* monkeys. J Neurophysiol 1996b;76:2754–2771. [PubMed: 8899643]

Tian JR, Lynch JC. Subcortical input to the smooth and saccadic eye movement subregions of the frontal eye field in *Cebus* monkey. J Neurosci 1997;17:9233–9247. [PubMed: 9364070]

Yan YJ, Cui DM, Lynch JC. Efferent targets of the pursuit subregion of the frontal eye field in *Cebus* monkey include the superior colliculus, pontine nuclei, and caudate nucleus. Soc Neurosci Abstr 1999;25:1397.

Yan YJ, Cui DM, Lynch JC. Distrubution of pontine terminals from saccade and smooth pursuit subregions of frontal eye field in *Cebus* monkeys. Soc Neurosci Abstr 2001a;27:404.2.

Yan YJ, Cui DM, Lynch JC. Overlap of saccadic and pursuit eye movement systems in the brain stem reticular formation. J Neurophysiol 2001b;86:3056–3060. [PubMed: 11731560]

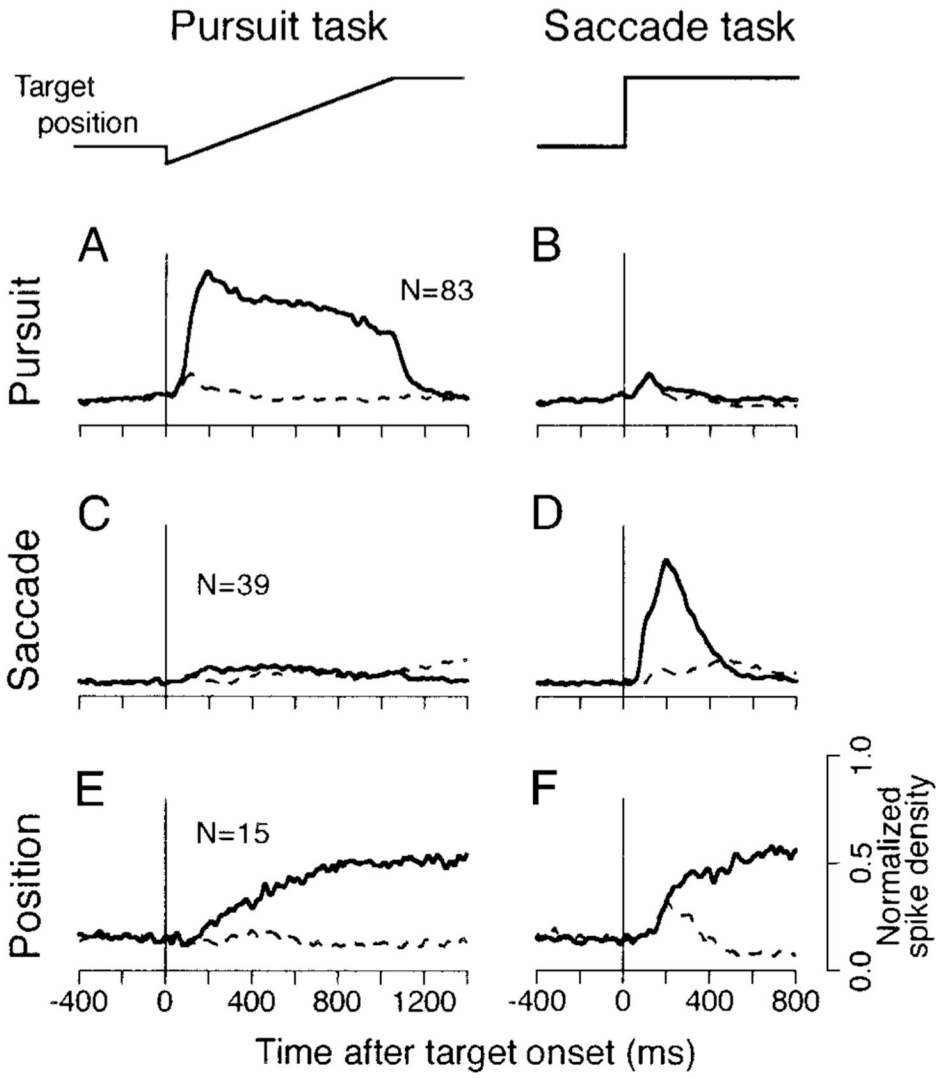


**FIG. 1. Qualitative definition of different neuronal types according to the time courses of population activity during different eye movement tasks**

Each pair of side-by-side traces plots mean of the normalized spike density of a single neuron type. The 2 columns show responses during the pursuit and saccade tasks. The traces labeled "target position" summarize the target motion for the 2 tasks. The solid traces indicate responses during eye movements in the cell's preferred direction, while the dashed traces indicate responses for the opposite direction. *A* and *B*: activity of pursuit cells. *C* and *D*: saccade cells. *E* and *F*: eye position cells. In pursuit trials, the target jumped 3–4° and moved in the opposite direction for 1,000 ms at 20°/s. In saccade trials, the target jumped 16°.

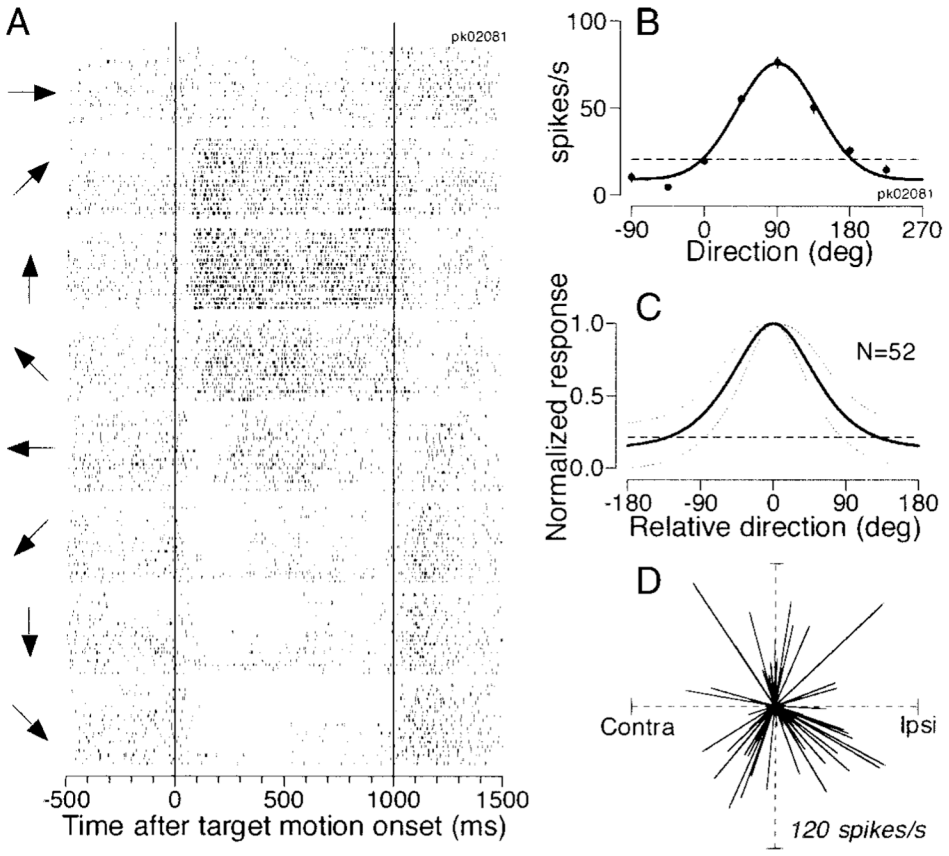


**FIG. 2. Quantitative analysis of direction tuning of pursuit neurons in the frontal pursuit area (FPA)**

*A*: raster display of a pursuit cell activity for 8 different pursuit directions. Two vertical lines indicate the onset and offset of target motion. The arrows at the *left* of each group of rasters indicate the directions of target motion. *B*: direction tuning for the cell shown in *A*. Each point plots the mean firing rate as a function of the direction of pursuit. The curve shows the result of fitting the points with a Gaussian function. Error bars show the SE, but are less that the diameters of the data points for most directions. The horizontal dashed line indicates baseline activity measured from 300 ms before target motion onset. *C*: the solid curve shows the normalized tuning averaged across 52 pursuit neurons. The dotted lines surrounding the tuning curve indicate 1 SD. *D*: each line represents a vector that starts at the center of the polar plot and shows the preferred direction and amplitude of modulation derived from the Gaussian function fitted to the direction tuning of each pursuit neuron.

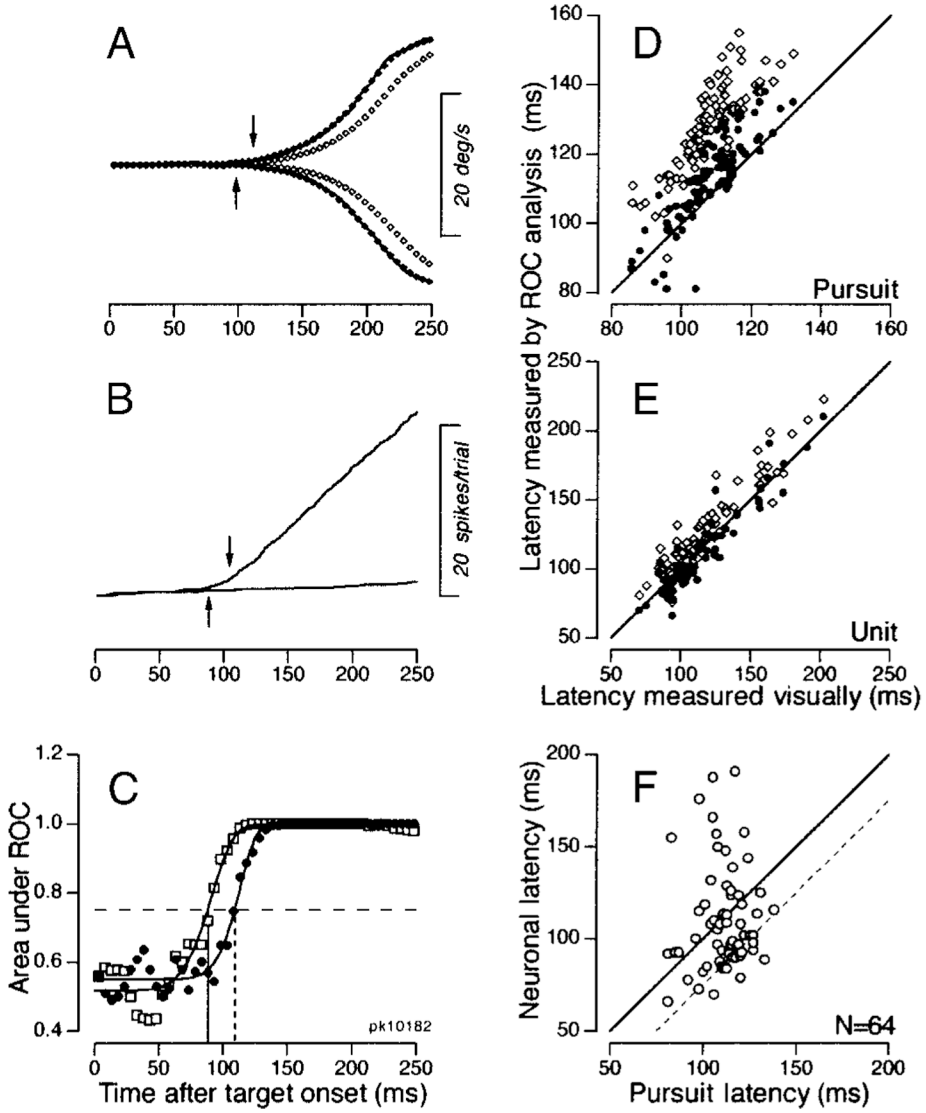


**FIG. 3. Analysis of latency difference between the neuronal responses in the FPA and the initiation of pursuit**

*A*: time course of component eye velocity along the preferred axis for the neuron under study. The filled and open symbols show eye velocity in 5-ms bins after applying a Gaussian or double-exponential filter, respectively. The continuous traces, hidden by the filled symbols, show millisecond-by-millisecond averages of eye velocity without any filtering. The upward and downward arrows indicate the onset of pursuit estimated by the receiver operating characteristics (ROC) analysis using the Gaussian and double-exponential filter, respectively. *B*: traces show the cumulative sum of spikes for pursuit in the preferred direction of the neuron under study and the opposite direction. The upward and downward arrows indicate the onset of a directional response in the neuron, estimated by the ROC analysis using the Gaussian and double-exponential filter, respectively. *C*: plot of the area under the ROC curves as a function of time. Filled and open symbols plot the data for eye velocity and neuronal firing shown in *A* and *B*, respectively. Curves indicate the best-fitting Weibul function, and the horizontal dashed line indicates the latency criterion of 0.75. *D* and *E*: comparison of latencies measured by the ROC analysis with those measured visually for the pursuit response (*D*) and for the

neuronal response (*E*). The ROC analysis using 2 different filters provided 2 symbols for each experiment. Open and filled symbols plot estimates of latency from the double-exponential and Gaussian filters, respectively. *F*: comparison of the neuronal and pursuit latencies estimated by the ROC analysis using Gaussian filter. The solid line has a slope of 1 and represents the situation where the pursuit and neuronal latencies were the same. The dashed line is shifted by 25 ms and represents the situation where the neuronal response preceded the initiation of pursuit by 25 ms. One outlier point has been omitted ([99, 210]).

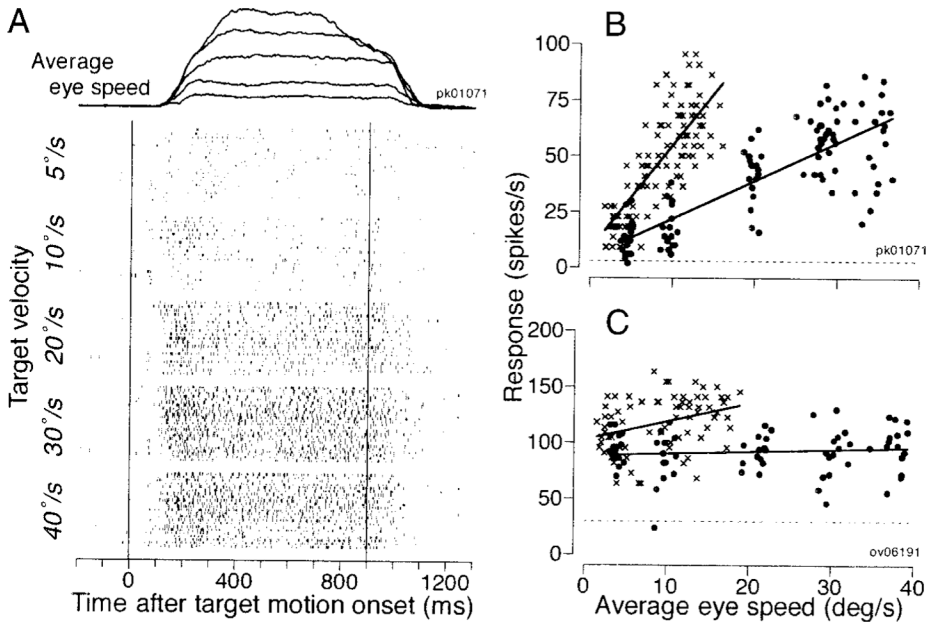


**FIG. 4. Eye velocity sensitivity in 2 representative FPA neurons**

*A*: the traces at the *top of the panel* show superimposed records of the eye speed in response to target motion at 5, 10, 20, 30, and 40°/s in the preferred direction of the neuron under study. The rasters summarize the responses of 1 neuron for the same speeds. Numbers to the *left* of each group of rasters indicate target speed. The 2 vertical lines indicate the interval when the target moved, to the left and downward in this example. *B* and *C*: quantitative data from 2 neurons. Each point plots neuronal firing rate as a function of average eye speed for an individual trial. X's show measurements from a 250-ms period starting from 50 ms after target motion onset. Filled symbols show measurements from a 500-ms period starting from 400 ms after target motion onset. The continuous lines through the data were obtained by linear regression on the values represented by the 2 symbols. The horizontal dashed lines indicate baseline activity measured for a 300-ms period before target motion onset.

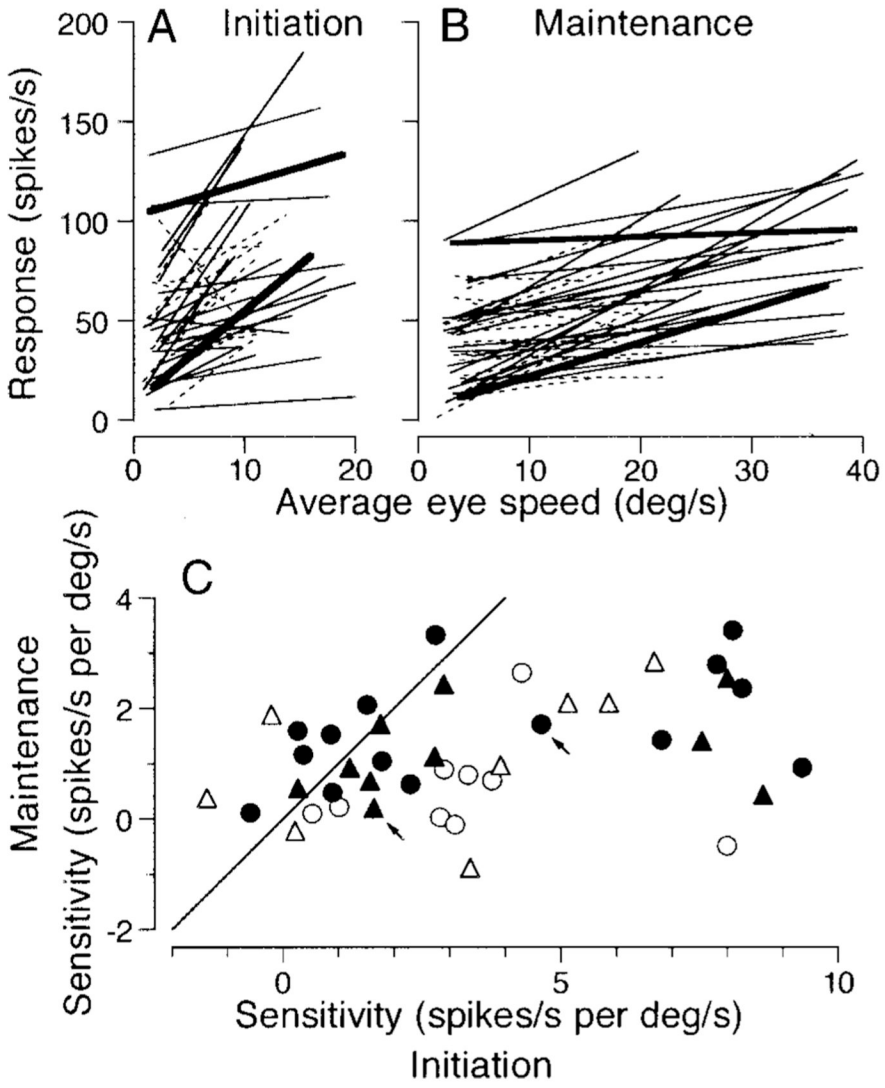


**FIG. 5. Quantitative summary of the eye velocity sensitivity of FPA neurons**

*A* and *B*: regression lines summarizing the sensitivity of 43 FPA pursuit neurons to eye velocity at the initiation (*A*) and maintenance (*B*) of pursuit. Continuous lines summarize data for 25 neurons examined for 5 different target velocities, while dashed lines show data for 18 cells tested only for 3 target velocities. Bold lines correspond to the neurons that provided the data shown in Fig. 4. In *A*, data from 1 neuron were above the range of the plot and have been omitted. *C*: comparison of the eye velocity sensitivity measured during the maintenance of pursuit and at the initiation of pursuit. Each symbol plots data from a different neuron. Filled and open symbols indicate data from cells examined for 5 or 3 different target velocities, respectively. Triangles indicate data from the neurons that showed directional modulation of firing rate more than 15 ms before the initiation of pursuit. Arrows point to the symbols for the 2 neurons that provide the data shown in Fig. 4.

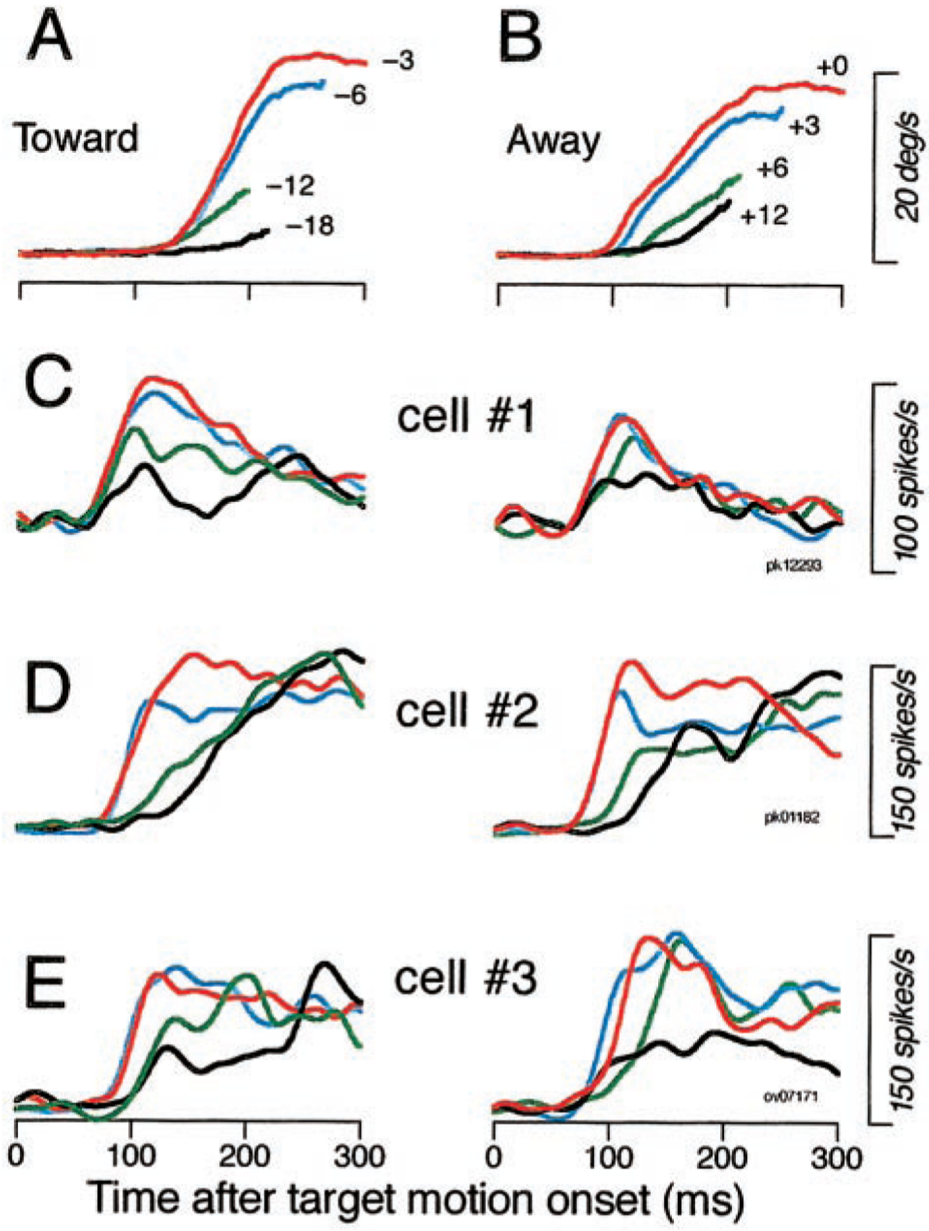


**FIG. 6. Parallel effects of the initial position of the moving target on the initiation of pursuit and the responses of FPA pursuit neurons**

*A* and *B*: traces show the time course of eye velocity during recording from *cell 1*. Different colors indicate different initial target positions, given by the numbers at the end of the traces. Results for target motion toward (*A*) or away (*B*) from the position of initial fixation are shown separately. Motion was always in the preferred direction of the neuron under study at 20°/s. The traces have varying lengths because they were truncated at different times by the 1st tracking saccades. *C–E*: time course of spike density for 3 neurons. Different color traces indicate different initial target positions according to the values given in *A* and *B*.

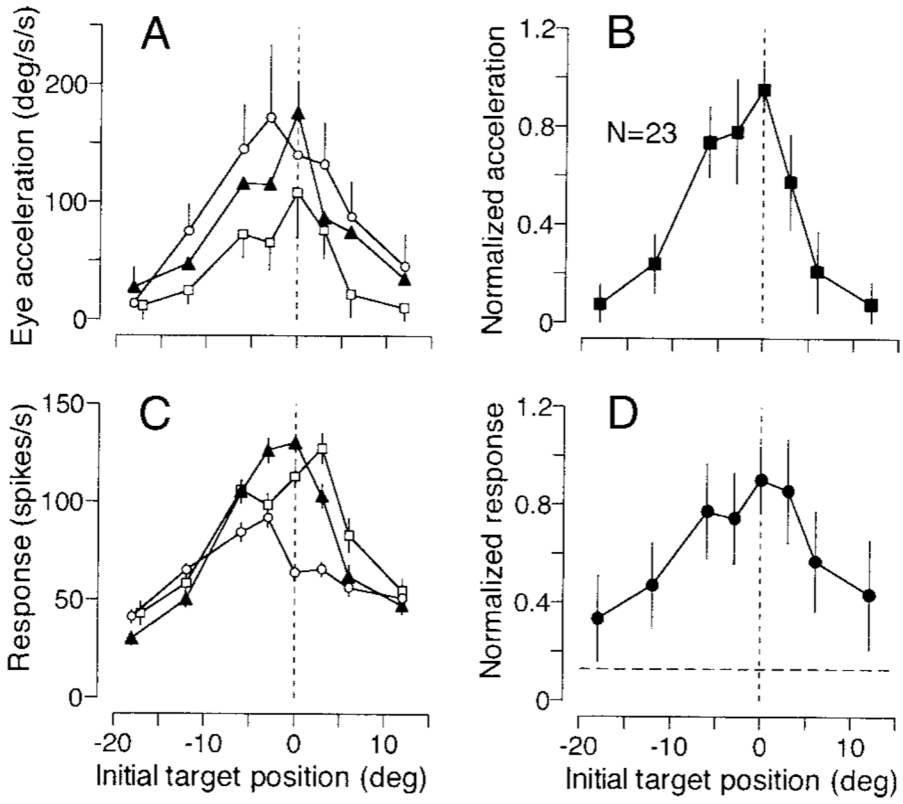


**FIG. 7. Quantitative analysis of parallel effects of the initial position of the moving target on the initiation of pursuit and the responses of FPA pursuit neurons**

*A*: initial eye acceleration measured from 121–180 ms after target motion onset is plotted as a function of initial target position for the 3 different recording experiments from Fig. 6. Error bars are shown only for a subset of data points to avoid overlap. *B*: summary of 23 experiments, showing averages of normalized eye acceleration as a function of initial target position. *C*: firing rate in the interval 91–180 ms after target motion onset is plotted as a function of initial target position for the same 3 experiments shown in *A*. *D*: summary of 23 experiments, showing averages of normalized neuronal activity as a function of initial target position. The horizontal dashed line indicates mean baseline activity measured from the 300-ms interval before target motion onset. Error bars indicate either 1 SE of the measurements from individual neurons (*A* and *C*) or 1 SD of the means across the population (*B* and *D*). In all 4 graphs, negative and positive values of initial target position correspond to trials in which the ramp of target motion moved the target toward and away from the position of fixation, respectively.

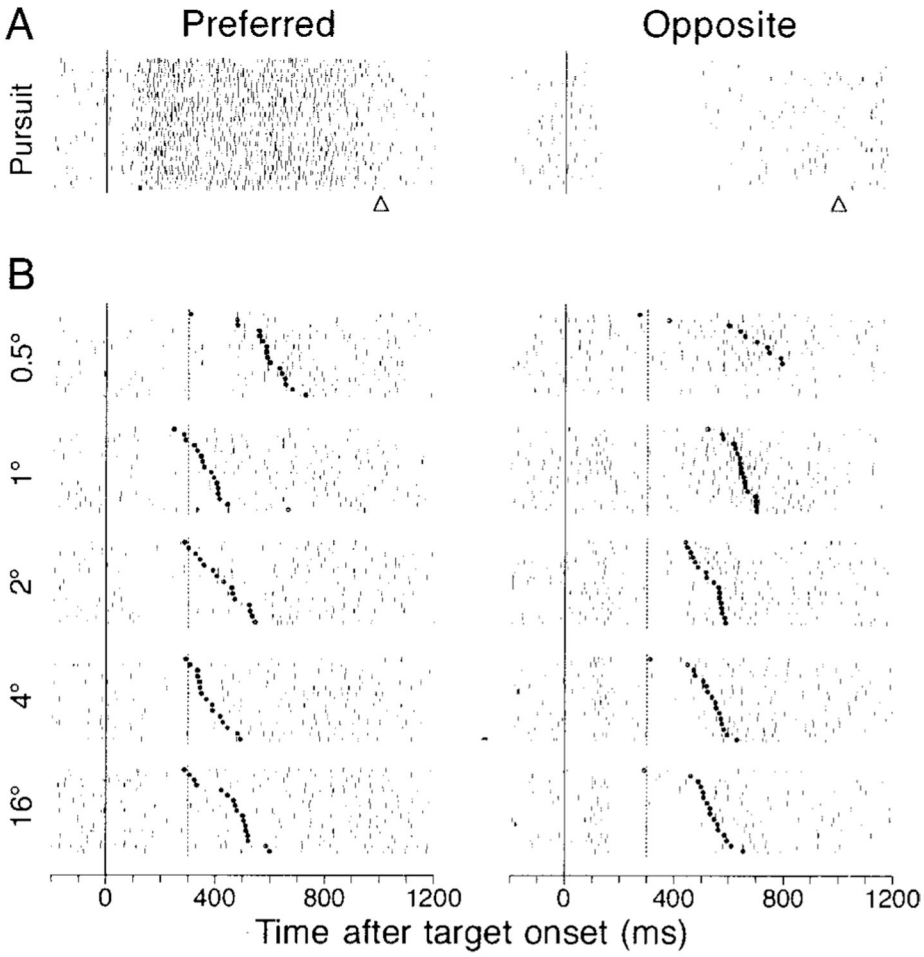


**FIG. 8. Responses to steps of target position and saccades in a representative pursuit neuron**

Each group of rasters shows the responses to a multiple repetitions of a trial. The *left* and *right columns* show responses during pursuit (*A*) or saccades (*B*) in the preferred direction of the neuron under study and the opposite direction, respectively. Preferred direction for this neuron was downward. From *top* to *bottom*, the target motions were step-ramps with 4° steps and 20°/s ramps, and target steps of 0.5, 1, 2, 4, and 16°. The continuous vertical lines show the onset of target motion (*A*) or the time of the target step (*B*). In the pursuit trials (*A*), the triangles below rasters indicate the time of target motion offset. In the saccade trials (*B*), the vertical dashed lines show the time when the fixation target was extinguished in the overlap task, and the bold dots show the time of saccade initiation. Within each group, trials have been ordered according to saccade latency.

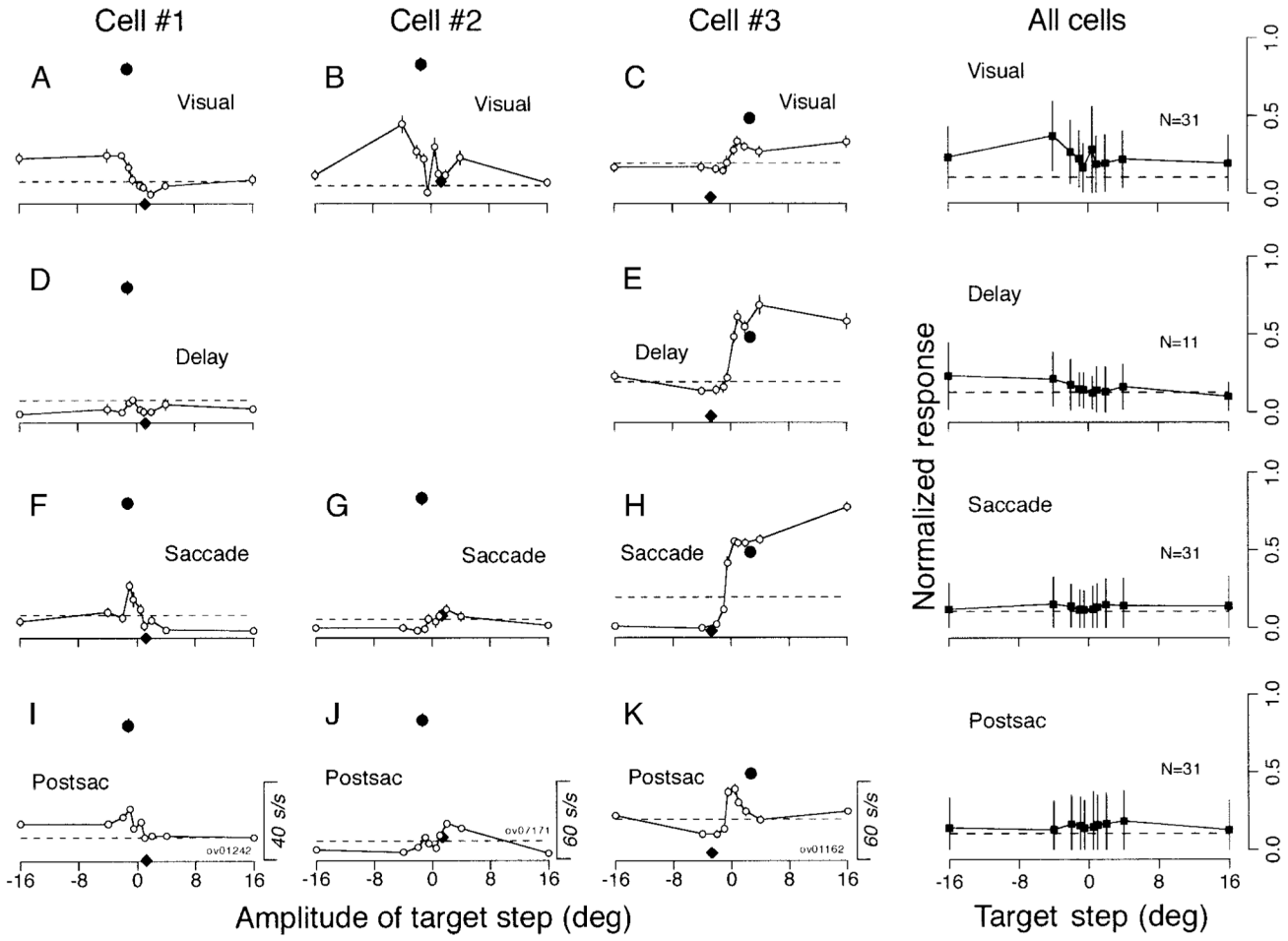


**FIG. 9. Quantitative summary of responses of FPA pursuit neurons during steps of target position and saccades**

The *left-hand 3 columns* summarize responses of 3 pursuit neurons, and the *right column* shows averages across all pursuit neurons with responses like those in *cells 1* and *2*. *Cell 1* in this figure depicts data from the cell shown in Fig. 8. *A–K*: the open symbols in each graph plot the mean and SE of neuronal response as a function of the amplitude of the target step, and different rows show data from different task intervals. *Row 1*: 80-ms period starting from 90 ms after target onset (Visual, *A–C*). *Row 2*: the period starting from 180 ms after target onset to 50 ms before saccade onset (Delay, *D* and *E*), *Row 3*: 80-ms period starting from 40 ms before saccade onset (Saccade, *F–H*). *Row 4*: 80-ms period after saccade offset (Postsac, *I–K*). The filled circle plots the maximal value of the mean firing rate during pursuit within any 80-ms interval as a function of retinal position of target image 80 ms before the measuring interval. The black diamond indicates response at the same task interval but during pursuit in the opposite direction. The measurement intervals of the neuronal activity for the *cells 1–3* started 180, 122, and 376 ms after target motion onset, respectively. Horizontal dashed lines indicate baseline activity during the 300 ms before the step of target position. The column labeled “All cells” plots the mean and SD of the normalized responses to target steps across our sample of neurons. Positive values along the abscissa indicate the preferred direction for pursuit.

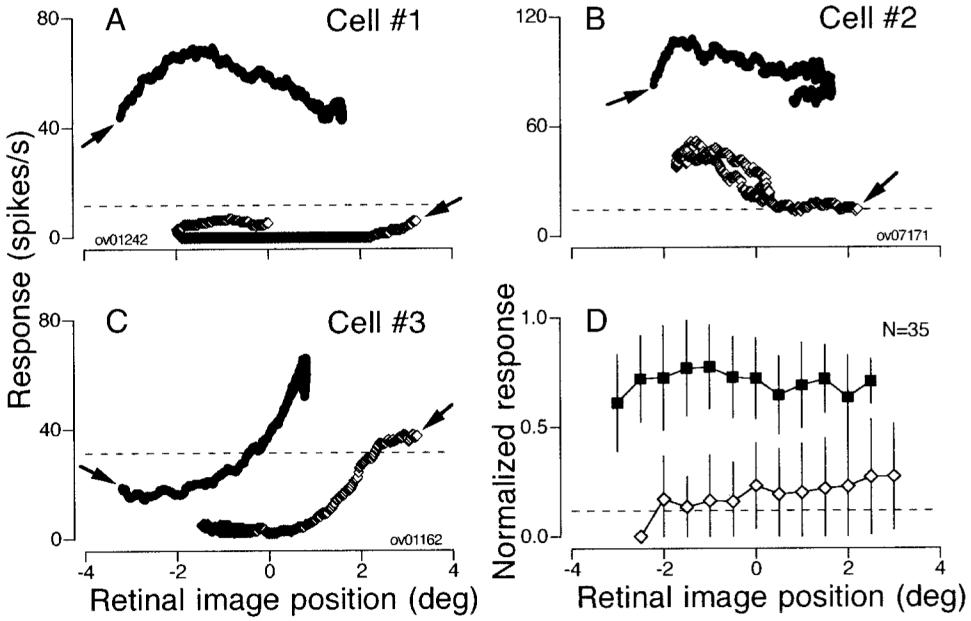


**FIG. 10. Activity during pursuit as a function of retinal position of target images**

*A–C*: data for 3 cells same as shown in Fig. 9. The symbols in each graph plot the mean firing rate during all 80-ms intervals as a function of mean retinal position error measured 80 ms earlier. One point is plotted for each 1-ms time step from 80–600 ms after target motion onset. Filled and open symbols plot data for pursuit in the preferred and the opposite direction. The arrows indicate the data for the 1st measurement interval for each direction of target motion. Horizontal dashed lines indicate baseline activity. *D*: mean and SD of the normalized response is plotted as a function of retinal position error for 35 pursuit neurons. Data from all neurons were normalized, and then grouped and averaged within 0.5° bins of retinal position error. Filled and open symbols plot responses for pursuit in the preferred direction and the opposite direction.

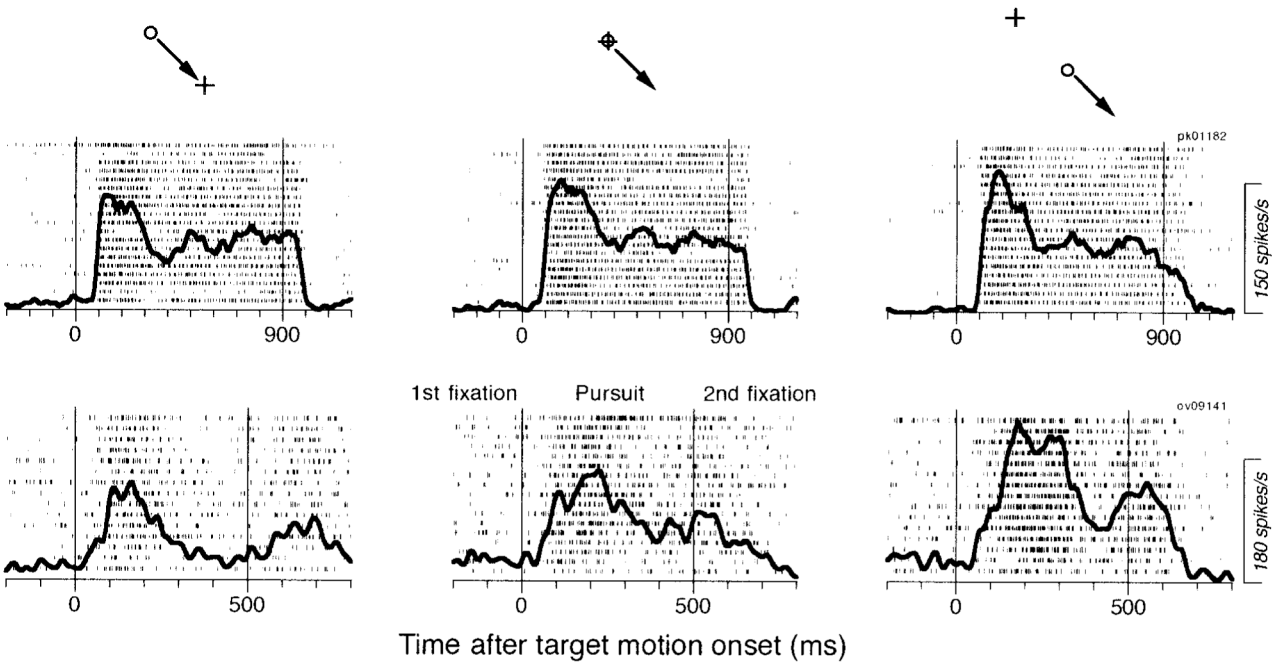


**FIG. 11. Sensitivity of pursuit responses to orbital eye position in 2 FPA pursuit neurons**

The *insets* above each column indicate the target configuration, with the circle showing the location of the moving target, the arrow indicating the direction of target motion, and the plus sign showing the center of the screen. The 2 rows of rasters show data from 2 neurons. Each raster shows the responses to multiple repetitions of the target configuration indicated by the *inset* at the *top* of the column. The bold trace shows the average spike density. The 2 vertical lines indicate the onset and offset of target motion. The target was visible and stationary before and after the motion interval, and the animals were required to fixate the target during those periods. The responses of the cell in *top row* were tested for right and downward pursuit, whereas those in *bottom row* were tested for downward pursuit.

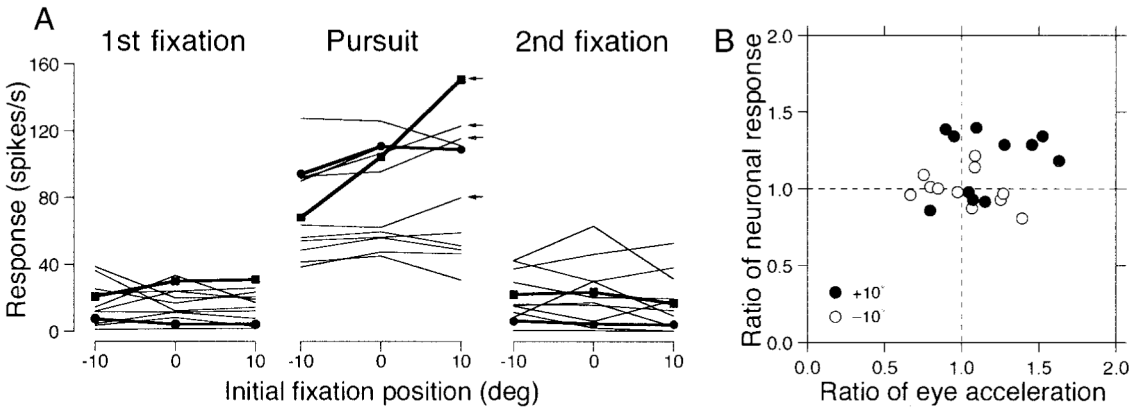


**FIG. 12. Quantitative summary of the effect of orbital position on the responses of FPA pursuit neurons**

*A*: each set of connected points shows data from 1 neuron, and each symbol plots average firing rate as a function of the initial orbital position of the eye at the start of the same step-ramp target motion. From *left* to *right*, the 3 graphs show data for 3 measurement intervals: 300 ms before target motion onset (*1st fixation*); 400-ms interval starting 100 ms after target motion onset (*Pursuit*); and 300-ms interval starting from 300 ms after target motion offset (*2nd fixation*). Positive values on the abscissa indicate fixation orbital positions in the preferred pursuit direction of the neuron under study. Filled symbols and bold lines show the data for the example neurons used in Fig. 11. The 4 small arrows at the right of the pursuit graph indicate the 4 neurons with regression slopes > 1.0. *B*: each symbol summarizes the responses of 1 neuron and plots the neuronal activity as a function of eye acceleration during the initiation of pursuit. Filled and open symbols plot data for initial orbital positions at −10 or +10° relative to the center of the screen along the preferred axis of the neuron under study. Both the neuronal activity and eye acceleration for trials with eccentric starting locations (±10°) were normalized for the responses in pursuit trials that started with central fixation.

**TABLE 1**

Number of cells examined in this study

| Monkey and Hemisphere | Cell Types | | | | |
|---|---|---|---|---|---|
| | **Pursuit** | **Saccade** | **Position** | **Others** | **Total** |
| *PCK*, right | 34 | 23 | 12 | 2 | 71 (43) |
| *OLV*, right | 43 | 8 | 2 | 4 | 57 (34) |
| *OLV*, left | 13 | 11 | 2 | 12 | 38 (23) |
| Total | 90 (54) | 42 (25) | 16 (10) | 18 (11) | 166 (100) |

Numbers in parentheses are percentages.